Technische Universität München
Fakultät für Medizin

The role of aldehyde dehydrogenase 1 in the combined treatment of glioma cells with cold atmospheric plasma and standard radiotherapy

Alicia Gantzkow

Vollständiger Abdruck der von der Fakultät für Medizin der Technischen Universität München zur Erlangung des akademischen Grades einer Doktorin der Medizin (Dr. med.) genehmigten Dissertation.

Vorsitz: apl. Prof. Dr. Bernhard Haslinger

Prüfer*innen der Dissertation:

1. Prof. Dr. Jürgen Schlegel
2. Priv.-Doz. Dr. Friederike Liesche-Starnecker

Die Dissertation wurde am 21.07.2022 bei der Technischen Universität München eingereicht und durch die Fakultät für Medizin am 13.12.2022 angenommen.

Table of contents

Abbreviations

ALDH1	Aldehyde dehydrogenase isoform 1
CAP	Cold atmospheric plasma
CNS	Central nervous system
DBD	Dielectric barrier discharge
DEAB	Diethylaminobenztaldehyde
DMEM	Dulbecco's Modified Eagle's Medium
DSF	Disulfiram
FBS	Fetal bovine serum
GBM	Glioblastoma multiforme
hr	hour
IDH	Isocytrate Dehydrogenase
IF	Immunofluorescence
IR	Irradiation
LPO	Lipid Peroxidation
MTT	3-(4,5-dimethylthiazol-2-yl)-2,5-diphenyl-tetrazolium bromide
MGMT	O6-methylguanin-DNA methyltransferase
NAC	N-acetyl cysteine
o.n.	over night
rcf	relative centrifugal force
ROS	Reactive Oxygen Species
rpm	revolutions per minute
RT	room temperature

sec	second
SDS-PAGE	Sodium dodecyl sulfate-polyacrylamide gel electrophoresis
WHO	World Health Organization
Wt	Wild type

List of figures

List of tables

1 Introduction

1.1 Glioblastoma multiforme

1.1.1 Etiology and Epidemiology

Glioblastoma multiforme (GBM) is the most common and lethal of malignant brain tumors in adulthood. It accounts for 67 – 68 % of all malignant brain tumors in adults in Germany (Robert Koch-Institut, 2019). According to the World Health Organization (WHO), GBMs are classified as WHO CNS grade 4 tumors and occur most frequently in patients over 55 years of age.

The etiology of GBM remains largely unknown. The only proven risk factor is ionizing radiation. Furthermore, some rare genetic disorders – as Turcot syndrome and neurofibromatosis type I and II – are related to higher incidence rates of glial tumors. (Schwartzbaum et al., 2006).

There is no specific data regarding the incidence of GBM in Germany as most studies present combined statistics for several cancers of the central nervous system (CNS). Data for the United States show an incidence of GBM of 3.23 per 100.000 and a slightly more frequent occurrence in men (Ostrom et al., 2021). Until today GBM remains one of the tumor entities with the poorest overall prognosis and a median survival of 14,6 months despite maximum therapy (Stupp et al., 2009). Only 6,8% of patients survive beyond 5 years (Ostrom et al., 2021). Although systemic metastasis almost never occurs, long-time survival rates remain very low due to therapy resistance and extremely high rates of recurrence (Ellis et al., 2015).

1.1.2 Diagnostic and therapeutic approach

GBMs can manifest with highly variable neurological deficits depending on their localization. Epileptic seizures or changes of nature are frequent, while symptoms of cerebral pressure such as headaches, nausea, vomiting, and congestion papillae often occur due to rapid tumor growth (Lapointe et al., 2018).

In MR images (T2 weighting) GBMs typically present as an inhomogeneous mass with strongly space-consuming character and ring-shaped contrast enhancement. MR spectroscopy may provide complementary information on tumor metabolites in selected cases, but histopathologic examination remains the gold standard for diagnosis and molecular characterization. Diagnosis is carried out in an integrated manner, combining molecular gene expression profiles and histological classification, thereby following the 2021 WHO classification as well as the recommendations of the cIMPACT-NOW consortium (Brat et al., 2020; Louis et al., 2021).

Therapy should be carried out as fast as possible. Standard treatment consists of surgical resection as complete as possible, followed by combined radiochemotherapy with the alkylating agent temozolomide (TMZ) and subsequently 6 cycles of maintenance chemotherapy with TMZ (Wick et al., 2021). In line with the recommended radiotherapy regime, a total dose of 60 Gy in 30 daily fractions of 2 Gy should be delivered (Stupp et al., 2009). Regarding surgical resection, fluorescence-guided resection improves the rate of complete resection as well as progression-free survival after 6 months (Stummer et al., 2006). Anyhow, avoiding new permanent neurological deficits has priority over surgical radicality. If inoperable, a stereotactic biopsy with integrated diagnosis should be performed. Additional treatment with tumor treating fields can be considered as it improves progression-free and overall survival for patients with newly diagnosed glioblastoma after completed radiochemotherapy and stable follow-up (Stupp et al., 2017). MRI check-ups should be performed every 3 months, or earlier if progression is suspected. There is no standard evidence-based therapy for the occurrence of progression. The current therapy should be terminated and a new therapy concept including reoperation, a renewed radio/chemotherapy as well as therapeutic approaches within the scope of clinical studies should be discussed individually (Wick et al., 2021). Adjusted treatment regimens – such as short-course radiotherapy – apply to older patients or patients with limited clinical functional status (Perry et al., 2017).

1.1.3 Classification of subtypes

The former distinction into subtypes (primary and secondary GBMs) has been revised by *The 2021 WHO Classification of Tumors of the Central Nervous System*. To reflect the differences according to IDH status (in particular, the significantly longer survival time of IDH-mutated tumors), only gliomas of IDH-wild type that meet the corresponding histologic criteria such as microvascular proliferation and/or necrosis are now still referred to as glioblastoma. Tumors previously classified as GBM, IDH-mutated, are now labeled as astrocytoma, IDH-mutated, WHO CNS grade 4 (Louis et al., 2021). However, due to the previous classification not yet available studies, these should continue to be treated analogously to GBM, IDH wild-type, or IDH-mutated astrocytoma, WHO CNS grade 3 (Brat et al., 2020).

1.1.4 Mechanisms of therapy resistance

Unfortunately, the efficacy of treatment is limited by therapy resistance and inevitable tumor relapse. Despite intensive research in recent years on understanding the molecular basis of GBM, the underlying mechanisms remain largely unknown. Within the genetic factors identified, the methylation of the methylguanine transferase (MGMT) gene promotor indicates a more favorable prognosis and acts as a predictive marker for response to alkylating chemotherapy (Hegi et al., 2008; Louis et al., 2016). However, there is no consensus to omit chemotherapy in cases of unmethylated MGMT gene promotor, as moderate effects of TMZ have been shown even in this patient population (Perry et al., 2017). Obstacles in the treatment of GBM include inter- and intratumor heterogeneity, invasive growth character of diffuse gliomas, poor drug delivery across the blood-brain barrier, as well as the absence of established biomarkers (Ellis et al., 2015; Giese & Westphal, 2001). Furthermore, cancer stem cells (CSC) are discussed as a possible driver of treatment resistance. These CSCs are mainly found in hypoxic areas, are less sensitive to reactive oxygen species (ROS) and seem to escape standard therapy. (Heddleston et al. 2009, Soehngen et al. 2014).

1.2 Cold Atmospheric Plasma

Plasma is the fourth fundamental state of matter after solid, liquid, and gaseous. It is defined as an ionized gas that is quasi-neutral, as it contains equal numbers of negative and positive charged particles. The resulting highly reactive mix of ions and electrons, and reactive molecules is generated in a strong electric field and is normally associated with enormous heat production. Plasmas have been widely used in medicine including applications such as sterilization, disinfection, and cauterization (Ayliffe, 2000; Venkatesh & Ramanujam, 2002). However, their use on human tissue has been restricted due to their high temperatures. In recent years, progress has been made in plasma physics which has enabled the generation of CAP at atmospheric pressure on earth. This achievement has paved the way for new biomedical implementations including in vivo applications that can be performed painlessly and are gentle on the surrounding tissue (Fridman et al., 2008; Isbary et al., 2013).

For the generation of CAP, different CAP devices are available based on two different approaches: indirect discharges using a plasma jet or direct discharges using a dielectric barrier discharge (DBD). Both devices use similar physical principles, components and materials and generate plasma between an anode and a cathode. The Plasma Jet additionally requires a carrier gas for the formation of CAP, while the DBD device can generate CAP directly in air, but must be sufficiently close to the sample, since the latter acts as a second electrode and is thus an active part of the discharge (Yan et al., 2017).

1.2.1 Anti-cancer properties of CAP

The results of several studies – in vivo as well as in vitro – have raised hopes that CAP may represent an interesting new therapeutic option for the treatment of cancer. CAP has been shown to be more effective than the corresponding standard treatment in several cancer cell lines (Choi et al., 2017; Walk et al., 2013). Although the various cellular mechanisms involved are not fully understood, the production of reactive species, mainly ROS, is thought to play a central role.

Noticeable rise of ROS selectively occurs in cancer cells rather than normal cells upon the same CAP treatment (Keidar et al., 2011). Different models to explain this selective anti-cancer capacity are currently being discussed: One model draws on the different ROS levels in normal and cancer cells (Szatrowski & Nathan, 1991). The ROS concentration in cancer cells could exceed a critical threshold faster due to the already elevated basal ROS levels (Trachootham et al., 2009). Another explanation relates to the property of cancer cells to express more AQPs on their cytoplasmic membranes which would make membrane diffusion easier for ROS (Yan et al., 2015).

In addition, there appear to be additive effects in combination therapy. Köritzer et al. were able to show that CAP treatment increases the sensitivity of GBM cells towards standard temozolomide therapy (Koritzer et al., 2013).

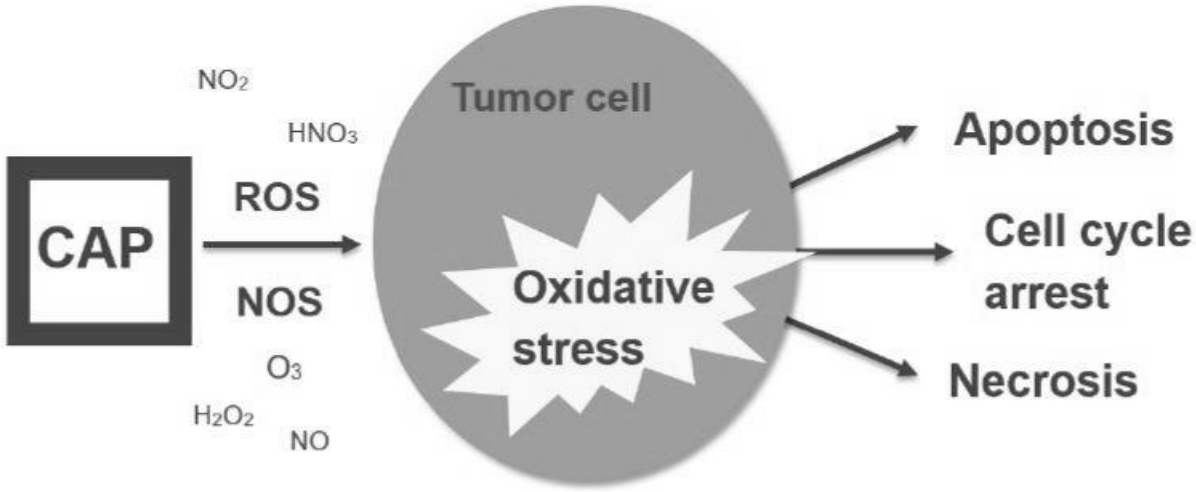

Figure 1: Effects of CAP

1.3 Aldehyde dehydrogenase (ALDH) isoenzymes

The human ALDH superfamily consists of to date known 19 NAD(P)+ dependent enzymes that hold a wide range of important physiological functions in the human body. Among other things, ALDH isoenzymes are involved in the biosynthesis of retinoic acids and are thus part of embryogenesis and differentiation as well as self-renewal of cells.

They are contributing to cellular detoxification and homeostasis by catalyzing the oxidation of endo- and exogenous aldehyde substrates to their corresponding carboxylic acids (Vasiliou et al., 1999; Vasiliou & Nebert, 2005). Endogenous aldehydes arise in the metabolism of amino acids, alcohol, or lipids. Exogenous aldehydes are generated by the metabolization of environmental substances and drugs (including chemotherapeutic agents). The ability of ALDHs to eliminate reactive aldehydes, including those derived from ROS-induced LPO, is thought to contribute to their functional role in carcinogenesis and treatment resistance (Marchitti et al., 2008).

ALDHs can be inhibited by various chemical agents. At this point, only disulfiram (DSF) will be discussed in more detail as this inhibitor was applied in the experiments below. DSF was originally used to treat alcoholism through accumulation of acetaldehyde and thereby creating alcohol aversion by unpleasant physiological consequences (Bell & Smith, 1949). Lately, various cancer cell models as well as in vivo experiments have been able to attribute an anti-cancer effect to DSF (Kim et al., 2016; Mao et al., 2013).

1.3.1 ALDH1 and Tumor Resistance

The isoenzyme ALDH1 is a member of the ALDH superfamily which is ubiquitously distributed in different tissues and cell types (Niederreither et al., 2002). ALDH1 has been suggested as a molecular marker for the identification of normal tissue stem cells (SC) as well as cancer stem cells (CSC) (Rasper et al., 2010). According to a theory of carcinogenesis first established in 1997, CSCs are a small subpopulation of cells within tumors that are capable of unlimited self-renewal (Bonnet & Dick, 1997). Although other cancer cells make up most of the mass of malignant cells, CSCs are thought to be the main culprit for treatment resistance, recurrence, and metastasis. In line with this, recent research could show that GBMs contain a small number of cells with stem cell properties that propagate regrowth after chemotherapy (Chen et al., 2012). The results of different research groups suggest ALDH isoenzymes as potential markers of CSCs as they are relatively highly expressed in drug-tolerant subpopulations of different tumor entities such as prostate cancer (Li et al., 2010), pancreatic cancer (Hermann et al., 2007), leukemia (Bonnet & Dick, 1997) and GBM (Rasper et al., 2010).

Furthermore, high activity and overexpression of ALDH1 are correlated with poor cancer prognosis and therapy resistance. Chen et al. postulated, that ALDH1 is associated with radio resistance of tumor cells (Chen et al., 2009). In addition, the findings of Schäfer et al. suggest that ALDH1 overexpression in glioma cells can provide protection against chemotherapy with TMZ (Schäfer et al., 2012).

1.4 Reactive Oxygen Species (ROS) and Lipid Peroxidation (LPO)

Reactive oxygen species (ROS) are produced as a natural by-product of various cellular processes, mainly by mitochondrial respiration and the activity of NADPH oxidases. ROS are produced by partial reduction of elemental oxygen and form a heterogeneous group of non-radical and radical oxygen compounds and are characterized by their high chemical reactivity, which can lead to oxidative damage of DNA, proteins, and lipids (Sies & Cadenas, 1985). Oxidative damage to lipids, known as lipid peroxidation (LPO), involves the formation of lipid radicals as well as disruptions in the structure cell membranes, leading to changes in permeability and consequent inhibition of metabolic processes. Additionally, LPO-induced mitochondrial dysfunction may lead to further ROS formation. Overall, the mentioned processes lead to a variety of breakdown products, most notably aldehydes, which can cause both cell cycle arrest as well as cell death (Barrera et al., 2008).

While low and medium ROS concentrations are involved in signal transduction, high cellular ROS concentrations have cytotoxic effects. The control of intracellular ROS is therefore of fundamental importance for maintaining cellular function. To ensure this, cells are equipped with extensive antioxidant protection mechanisms. Among those, the expression of antioxidant molecules such as glutathione is triggered via ROS-sensitive transcription factors, when the ROS concentration exceeds a certain threshold (Espinosa-Diez et al., 2015). The cumulation of ROS in times of uncontrolled production and inefficient elimination and the consecutive cellular oxidative stress and LPO play a crucial role in cell death as well as many pathological states and diseases such as inflammation, atherosclerosis, and cancer (Gupta et al., 2012).

1.5 Oxidative Stress in Cancer

Tumorigenesis is a multi-stage process defined by several phases: Initiation, Promotion, Latency, and Progression. ROS contribute to all these phases, as they not only damage DNA and trigger genetic dysregulation, such as activation of oncogenes and inactivation of tumor suppressor genes, but also significantly affect the characteristics of cancer cells by activating cellular signaling pathways. These signaling pathways regulate cell division, angiogenesis, and metastasis and thus contribute to cancer development (Moloney & Cotter, 2018). In addition, cancer cells are overall adapted to higher ROS concentrations and have higher antioxidant capacities (Pelicano et al., 2004).

On the other hand, the cytotoxicity of ROS has been used to inactivate cancer cells, as increased ROS concentrations can trigger programmed cell death. It has been suggested, that due to the already permanently elevated ROS concentrations, the precise fine-tuning between ROS production and recovery can be overturned more quickly (Trachootham et al., 2009). Indeed, common anti-cancer methods like chemo- and radiotherapy as well as newer approaches such as tyrosine kinase inhibitors cause apoptosis by induction of oxidative stress (Perillo et al., 2020).

In summary, ROS play a dual role in cancer development and control. This points to the urgent need to develop more therapeutic strategies to overwhelm the redox adaptation of cancer cells.

2 Aims of this study

GBM is one of the tumor entities with the poorest overall outcome, with the underlying mechanisms remaining unclear to date. Several studies suggested ALDH as a potential marker of cancer cells and demonstrated that overexpression of ALDH in GBM is associated with resistance to therapy. Recently, CAP has become available as a promising new treatment approach for cancer. Moreover, first studies indicated that CAP leads to enhanced efficacy of standard chemotherapy in a combinatorial approach.

The aim of the present project was to evaluate the cell biological basis of effects induced by CAP as well as by a combined treatment regimen.

To this end, C6 glioma cells were treated with CAP either alone or in combination with conventional IR. Since ALDH is induced by oxidative stress, the experiments were performed in the presence or absence of a ROS scavenger and an ALDH inhibitor.

MTT assay was used to investigate the treatment effects on proliferation and cell death and to elucidate whether CAP can improve the efficacy of standard radiotherapy in C6 glioma cells.

Western blot and immunofluorescence were performed to examine whether CAP alone or in combination with IR leads to a change in the expression of ALDH1A1 and ALDH1A3. ALDH enzyme activity was visualized using Aldefluor Assay to investigate whether ALDH is involved in the metabolism of oxidative stress products in C6 glioma cells.

All in all, this project thrived to unravel the role of ALDH1 for the treatment effects induced by CAP either alone or in combination with standard therapy.

3 Material and Methods

3.1 Material

3.1.1 Technical Devices

Device	Model	Producer
CAP device	DBD electrode	Terraplasma medical GmbH, Munich, Germany
Cell counter	Casy1	SchärfeSystem, Reutlingen, Germany
Centrifuge	5471R	Eppendorf AG, Hamburg, Germany
Centrifuge	4K15	Sigma, Deisenhofen, Germany
Cell culture incubator – 37°C, 5,2% CO_2	HERAcell 150i	Thermo Fisher Scientific Inc, Waltham, MA, USA
Electrophoresis cell	Mini-Protean tetra cell	BioRad Laboratories, Inc., Munich, Germany
Flow cytometer	FACS Calibur™	Becton Dickinson, Heidelberg, Germany
Fluorescence microscope	HBO 100	Carl Zeiss AG, Jena, Germany
Inverted routine microscope	Eclipse TS100	Nikon, Düsseldorf, Germany
Microplate reader	Infinite F200 Pro	Tecan Group Ltd., Männerdorf, Switzerland
Semi-dry transfer cell	Trans-Blot SD	BioRad Laboratories, Inc., Munich, Germany
X-ray film processor	Konica SRX-101A	Konica Minolta GmbH, Langenhagen, Germany
X-ray research irradiator cabinet	RS225	XStrahl Limited, Surrey, United Kingdom

Table 1: Technical Devices

3.1.2 Cell culture consumables and additives

Substances/Materials	Company
Cell culture dishes, 40mm	Sigma-Aldrich, Munich, Germany
Cell scraper	Greiner Bio-One GmbH, Frickenhausen, Germany
Microplate, 96 wells	Greiner Bio-One GmbH, Frickenhausen, Germany
Neubauer hemocytometer	VWR International GmbH, Darmstadt, Germany
Ibidi µl-Slides 8 chambers	Ibidi GmbH, Gräfelfing, Germany
T75 cell culture flasks	Thermo Fisher Scientific Inc., Waltham, USA

Table 2: Cell culture consumables and additives

3.1.3 Chemicals and Reagents

Substances	Abbreviation	Company
Acrylamide		Carl Roth GmbH + Co. KG, Karlsruhe, Germany
Aldefluor assay kit		STEMCELL Technologies, Cologne, Germany
Ammonium peroxodisulphate	APS	Carl Roth GmbH + Co. KG, Karlsruhe, Germany
Bovine serum albumin	BSA	Bio-Rad Laboratories, Inc., Munich, Germany
Chemiluminescence substrate	ECL	Millipore, Billerica, MA, USA
Autofluorescence Quenching Kit with DAPI (4′,6-Diamidin-2-phenylindol)		Vector Laboratories Inc., Burlingame, California, USA
Dimethyl sulfoxide	DMSO	Carl Roth GmbH + Co. KG, Karlsruhe, Germany
Dulbecco’s Modified Eagle’s Medium	DMEM	Thermo Fisher Scientific Inc., Waltham, USA

Fetal bovine serum	FBS	Biochrom AG, Berlin, Germany
Fumitremorgin C		Sigma Aldrich, Munich, Germany
Nitrocellulose membrane		Thermo Fisher Scientific Inc., Waltham, USA
N-acetyl-L-cysteine	NAC	Sigma-Aldrich, Munich, Germany
Page Ruler Plus		Thermo Fisher Scientific Inc., Waltham, USA
Phosphate buffered saline	PBS	Thermo Fisher Scientific Inc., Waltham, USA
Ponceau Red		Carl Roth GmbH + Co. KG, Karlsruhe, Germany
Protease phosphatase inhibitor		Cell Signaling Technologies, Frankfurt, Germany
Skimmed milk powder		Merck KG, Darmstadt, Germany
Sodium dodecyl sulfate	SDS	Carl Roth GmbH + Co. KG, Karlsruhe, Germany
Tetramethylethylendiamine	TEMED	Carl Roth GmbH + Co. KG, Karlsruhe, Germany
3-(4,5-dimethylthiazol-2-yl)-2,5-diphenyltetrazolium bromide	MTT	Carl Roth GmbH + Co. KG, Karlsruhe, Germany
Trypsin		Thermo Fisher Scientific Inc., Waltham, USA
Tris		Carl Roth GmbH + Co. KG, Karlsruhe, Germany
Tween20		Carl Roth GmbH + Co. KG, Karlsruhe, Germany
Verapamil		Sigma Aldrich, Munich, Germany

Table 3: Chemicals and Reagents

3.1.4 Solutions and Buffers

Solution/Buffer	Components	in
10x SDS running buffer	25mM Tris, 192µM Glycin, 0,5% SDS	ddH_2O
10x TBS buffer	20mM Tris, 150mM NaCl, pH 7,5 with HCl	ddH_2O
10x Transfer buffer	25mM Tris, 190mM glycine, 10g SDS, 200ml 96% ethanol	ddH_2O
5x Laemmli (Loading Dye)	60mM Tris-HCl (pH 6,8), 2% SDS, 10% Glycerol, 5% ß-mercaptoethanol, 0,01% bromophenol-blue	ddH_2O
BSA	5% BSA	T-BST
Cell lysis buffer	20% L-Buffer, 2%PMSF	
Immunofluorescence blocking buffer	1% BSA, 0,1% TX 100, 0,2% cold fish gelatin, 0,02% Sodium azide, 2,5% Horse Serum	PBS
RIPA-Buffer	10mM HEPES, 150mM NaCl, 2mM EDTA, 1% NP-40, 0,1% Triton X-100	ddH_2O
Tris Buffered Saline with Tween 20 (TBS-T)	10% TBS, 0,01% Tween20	ddH_2O
Western blot blocking buffer	TBS-T + 5% skimmed milk powder	

Table 4: Solutions and Buffers

3.1.5 Primary Antibodies

Name	Anti-ALDH1A1	Anti-ALDH1A3	Vinculin
Company	Abcam, Cambridge, USA	Abcam, Cambridge, USA	Abcam, Cambridge, USA

Isotype	Rabbit IgG	Rabbit IgG	Rabbit IgG
Molecular weight	55 kDa	55kDa	124 kDa
Dilution WB	1:1000, milk	1:1000, milk	1:30.000, milk
Dilution IF	1:500, blocking buffer	1:700, blocking buffer	

Table 5: Primary antibodies

3.1.6 Secondary Antibodies

Name	**Anti-rabbit (HRP-linked)**	**IF anti-rabbit Rhodamine**
Company	Abcam, Cambridge, USA	Thermo Fisher Scientific Inc., Waltham, USA
Dilution	1:10.000, milk	1:500

Table 6: Secondary antibodies

3.1.7 Software

Software	**Company**
Axiovision Rel. 4.8.	Carl Zeiss Microscopy, LLC, Thornwood, NY, USA
Flow cytometry analysis	FlowJo, Tree Star, Inc., Ashland, OR, USA
Magellan 7.1	Tecan Group Ltd., Männerdorf, Switzerland
NIS Elements F3.2	Nikon Instruments Inc., Melville, NY, USA
ImageJ	National Institute of Health, USA
Microsoft Office	Microsoft Corporation, Redmond, Washington, USA

Table 7: Software

3.2 Methods

3.2.1 Project outline

Rat C6 glioma cells were treated with CAP generated by a DBD electrode either alone or in combination with conventional irradiation. The effects on cell viability as well as on expression and activity of ALDH1 have been investigated using standard protocols including MTT assay, Western Blot, and Aldefluor assay. Since ROS play an important role in the transmission of the cellular effects induced by CAP all treatment experiments have been performed in the presence or absence of a ROS scavenger (NAC). To address the role of ALDH1 experiments were repeated after chemical inhibition by DSF. Hereafter, the individual methods will be explained in more detail.

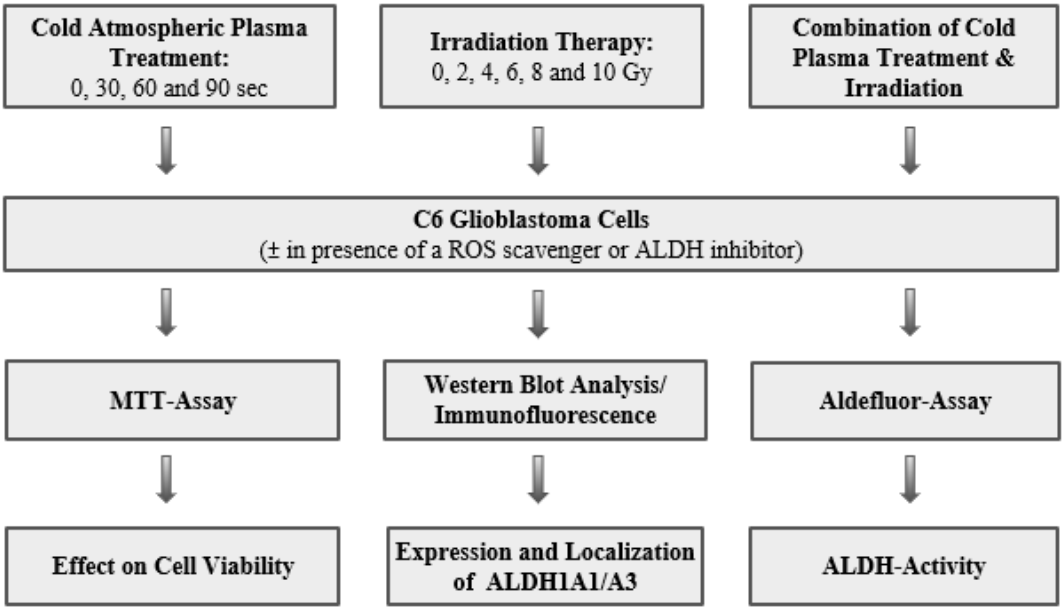

Figure 2: Experimental Setup (graph self-derived)

3.2.2 Cell Culture

C6 rat glioma cells (Table 8) were chosen with the prospect of subsequently connecting in vivo experiments on sufficiently large brains to the in vitro experiments. The cells were cultured in DMEM supplemented with 10 % FBS and cultivated in the presence of 5% CO_2 and 37°C in a humified incubator. They were passaged at an 80-100 % confluency every 2-3 days. Prior to treatment they were seeded in 40 mm plates with 2 ml of culture medium and let grow for 24 h to reach a monolayer with a confluency of 80 %.

Cell ID	**C6 (ATCC CCL-107)**
Company	ATTC
Organism	Rattus norvegicus (rat)
Tissue	Brain
Cell type	glial cell
Culture properties	adherent

Table 8: C6 cell line

3.2.3 CAP Treatment

The C6 cells were treated with CAP generated by a DBD electrode by terraplasma medical GmbH using the settings indicated below (Table 9). The medium was removed from the culture dishes before incubating the samples with CAP for either 0, 30, 60, or 90 sec.

Category	**Setting**
Voltage	3,5 kV
Frequency	4 kHz
Output	0,5 Watt
Distance	1,5cm

Table 9: CAP device settings

3.2.4 Irradiation

An RS225 X-Ray Box by X-Strahl Limited was used to irradiate the C6 cells. After evaluation of the effects of irradiation with 0 to 10 Gray, we selected sub-effective doses of irradiation (2 and 4 Gy) and CAP (30 sec) for combined treatment. The cells were irradiated 12 hours after application of CAP. All irradiation experiments were conducted using the settings indicated in Table 10.

Category	**Setting**
Voltage	200 kV
Amperage	15 mA
Filter	5 (Cu)
Height of table	488 mm
Duration of exposure	54 sec = 1 Gy

Table 10: Irradiation settings

3.2.5 MTT Assay

As only mitotic active cells metabolize the yellow tetrazolium salt MTT to purple formazan crystals, MTT assay provides the ability to assess the viability of cells. The recommendation by the manufacturer's manual was modified according to the use of 40 mm culture dishes. In brief, 24 and 48 h after treatment the culture medium was replaced by 2 ml of fresh medium, and 200 µl MTT was added. The samples were then incubated in darkness. After 4 hours the medium was removed, the cells were washed with PBS and the formazan crystals were solubilized in 2 ml of DMSO for 30 min. After the transfer of 100 µl of the suspension to each well of a 96-well-plate, absorbance was measured using a Tecan F200 Pro microplate reader at a wavelength of 595 nm.

3.2.6 SDS-Page and Western Blot

3.2.6.1 Protein Extraction

After adding 125 µl RIPA-Buffer supplemented with 0,02 % Protease Phosphatase Inhibitor the cells were scraped from the dish's surface and sonicated. The suspension was centrifuged by 20 000 rcf/ 14 000 rpm for 10 min at 4°C and the supernatant was transferred to a new vial. The total protein concentration was quantified by Bradford assay. After quantification, the protein lysate was mixed with 5x Laemmli buffer, boiled at 95 °C for 5 min subsequently spun down to promote denaturation. The protein lysate was stored at -20 °C.

3.2.6.2 SDS-Page

Polyacrylamide gels were prepared adjusted to protein size with a gel density of 10 %. After loading 25 µg of protein per lane, the separation was performed in SDS running buffer in an electrophoresis cell (BioRad Laboratories, Inc.). Separation was started at a Voltage of 100 V for 20 min and then increased to 200 V to finish the run in about one hour.

3.2.6.3 Wet Blotting/Protein Transfer

The gel sandwich cassette was prepared from anode to cathode with a filter paper, the nitrocellulose membrane, the polyacrylamide gel, and another filter paper, all completely submerged in Transfer Buffer. Transfer to the nitrocellulose membrane was then performed at 100 V for 1 hour in the electrode module.

3.2.6.4 Detection of Proteins

Ponceau Red solution was used to visualize the lanes before cutting the blots. Blocking of non-specific binding sites was performed in 5 % milk for 1 h. Antibodies were diluted as shown in the corresponding tables (Table 5; Table 6). The blots were incubated with primary antibodies o.n. at 4 °C. Subsequently binding of the secondary antibodies took place for 45 min at RT. Each of the steps mentioned was followed by washing with TBS-T. The blots were then covered with ECL substrate and the chemiluminescence was visualized with an X-ray film.

3.2.6.5 Relative Quantification of Western Blots using ImageJ

The scanned films, set to a greyscale, were examined for their "Grey Mean Value". The largest band in the corresponding protein row was used to define a framed region of interest. The same frame was used to measure all protein bands in the other lanes. These steps were repeated for loading control and background measurements. The data was then analyzed using Microsoft Excel. After inverting the pixel density for all data, the net data for each band was expressed by subtracting the background. A ratio of the net band value over net loading control was taken. For the final relative quantification values, the net band was ratioed to the net loading control.

3.2.7 Immunofluorescence

Immunofluorescence is an immunohistochemistry technique that is applied to visualize various cellular components such as proteins. Fluorophore-labeled secondary antibodies were utilized to detect primary antibodies coupled to the proteins of interest. Cells were seeded on an Ibidi chamber slide (Ibidi GmbH, Gräfelfing, Germany) 24 h before treatment. The culture medium was removed 24 h after treatment and cells were fixated with 4 % PFA for 15 min at 37 °C. Each step followed by washing with PBS, the samples were sequentially incubated with blocking buffer (20 min, RT), primary antibodies (o.n., 4 °C), and secondary antibodies (20 min, RT, in the dark). Staining with DAPI was applied for 10 min at RT in the dark before assessing the slides under the microscope.

3.2.8 Aldefluor Assay

ALDH activity in C6 cells was quantified using Aldefluor kit (Stemcell Technologies, Cologne, Germany) and FACS analysis. A single-cell suspension was prepared 24 h after CAP treatment. The suspension was spun down at 300 g for 5 min at RT and the supernatant was discharged. Prior to adding the Aldefluor assay buffer, the cell pellet was resuspended in DMEM supplemented with Verapamil and Fumitremorgin to inhibit ABC/PgG Transporters. Half of the untreated sample was mixed with DEAB to serve as a negative control. After incubation at +37 °C in the dark for 45 min, the sample was centrifugated at 300 g for 5 min at 4 °C. The cells were then resuspended in Aldefluor assay buffer and stored on ice up until FASC analysis. FlowJo software was used to analyse the data.

3.2.9 Statistical analysis

Results were plotted using Microsoft Excel software (Standard office 365 for Windows 10 Pro) as mean ± standard deviation. Data was considered significant for p values of less than 0.05 using a student t-test.

4 Results

4.1 Morphological effects

C6 glioma cells are multipolar fibroblast-like cells that grow in a monolayer attached to the cell culture dish's surface. Regular microscopic analyses were carried out to predict growth rate and to visualize the morphological changes in response to CAP treatment. Additionally, morphological assessment enabled the detection of possible errors at an early stage. A decrease in monolayer confluency with increasing CAP treatment times was observed, both 1 hour and 24 hours after treatment.

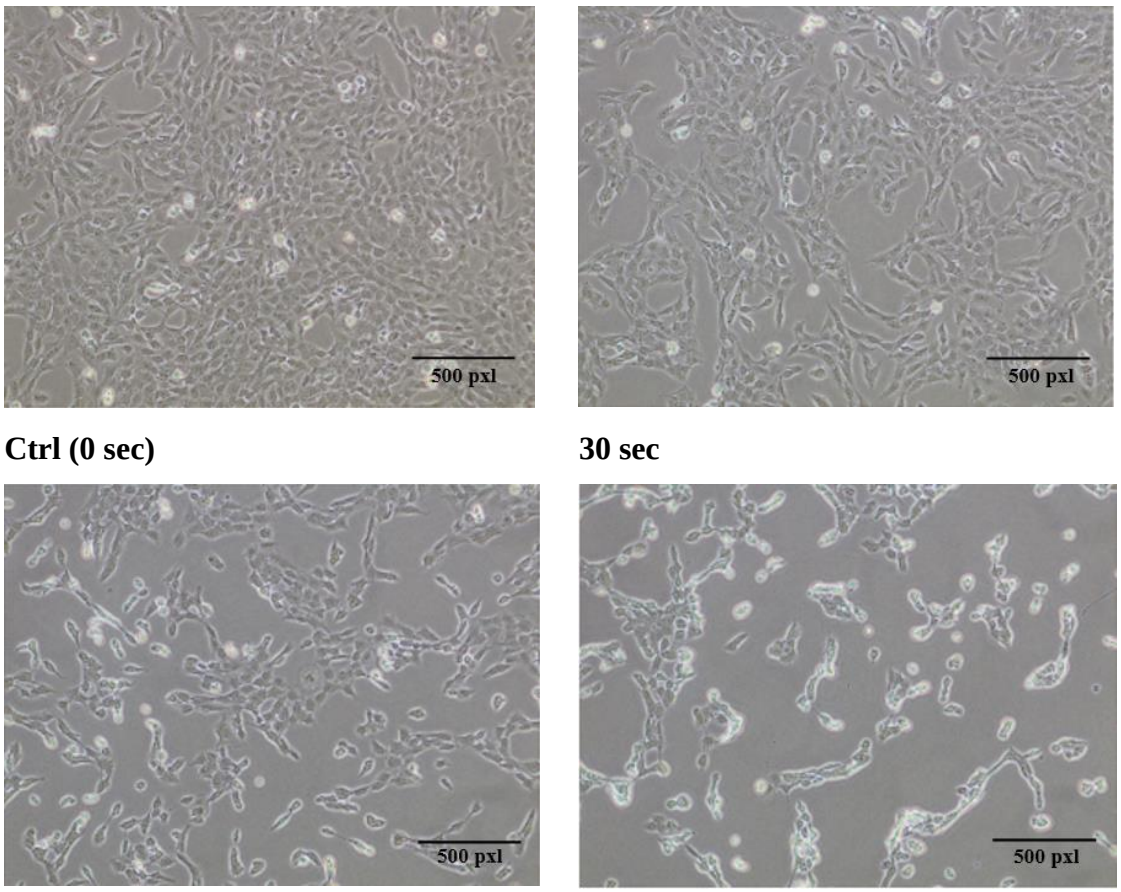

Ctrl (0 sec) **30 sec**

60 sec **90 sec**

Figure 3: Morphological effects 1 hour after CAP treatment. *C6 cells were incubated with CAP as described in Section 3.2.3 for different lengths of time (denoted in A, B, C, and D). Detached cells were observed in all samples, but with increasing quantity at longer treatment times. In addition to a significant decrease in cell confluency with longer treatment times, the cells underwent morphological changes towards contracted, smaller cells with a less elongated shape.*

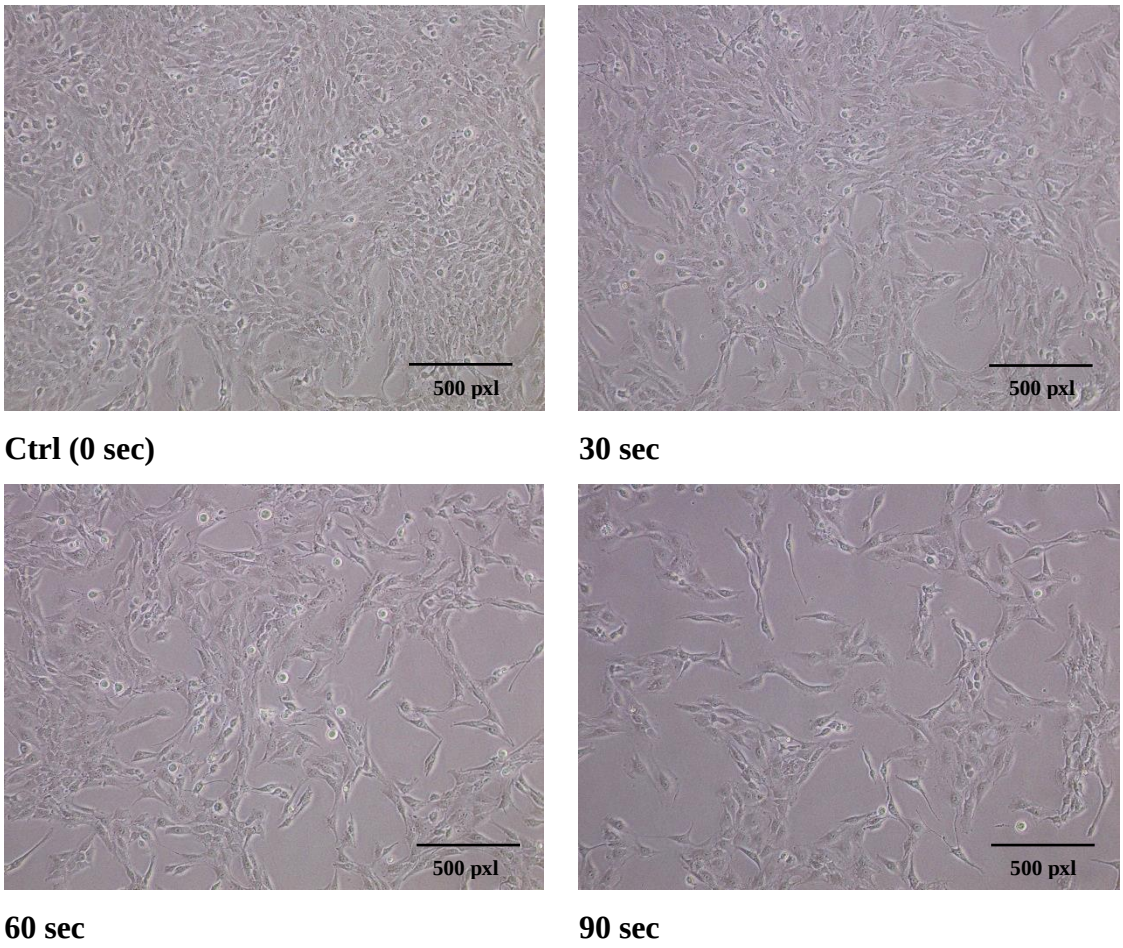

Figure 4: Morphological effects 24 hours after CAP treatment. *C6 cells were treated as indicated below Fig. 4. Compared to Fig. 4 less detached, floating cells were detected. With increasing treatment times, cell confluency decreased. The morphological changes observed 1 hour after treatment had mostly reverted to the initial state of fibroblast-like cells with only a few cells in the samples treated for 60 and 90 sec presenting in a round, retracted shape.*

4.2 Cell viability

4.2.1 Cell viability decreases after CAP treatment

In addition to morphological assessment, C6 cells were analyzed by MTT assay. Regarding the hypothesis, it was crucial to examine the effects on cell viability of different treatment options as well as identify sub-effective dosages of CAP and IR in order to design combined treatment experiments based on the results.

To determine which treatment duration was effective or sub-effective, C6 glioma cells were treated for different durations of 30, 60 and 90 sec. The MTT assay results showed that after 24 hours, slightly more than 70% cell viability remained for treatment times up to 60 sec, while after 90 sec, only less than 50% of the cells were still viable. The p-values for all treatment times were statistically significant compared to the control. The sub-effective doses for the combined treatment with radiotherapy were therefore set at 30 and 60 sec.

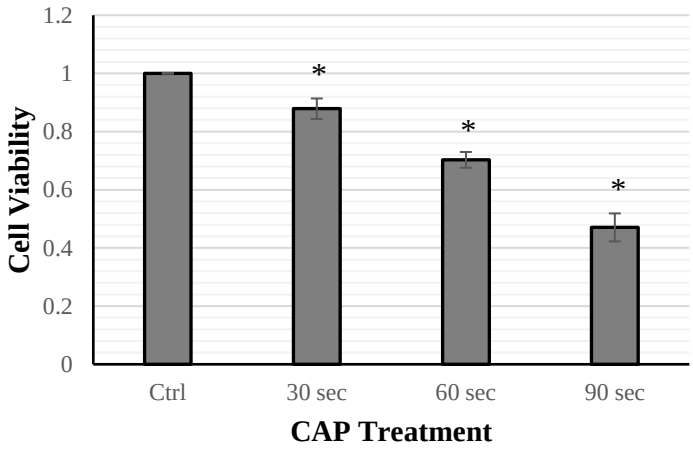

Figure 5: Cell viability 24h after CAP treatment. *C6 glioma cells were incubated with CAP as described in Section 3.2.3. Fresh medium was added directly after CAP treatment. The graph is based on the mean value of four samples. The asterisk indicates statistical significance compared to the untreated control.*

4.2.2 NAC can mitigate CAP effects on C6 cells

Since ROS are thought to be the key player in the transmission of cellular effects induced by CAP, all treatment experiments were performed again in the presence of the ROS-Scavenger NAC. The addition of NAC almost completely blocked the effect of CAP up to a treatment time of 60 sec. With a treatment duration of 90 seconds, the effect could no longer be blocked completely, but still to a significant extent.

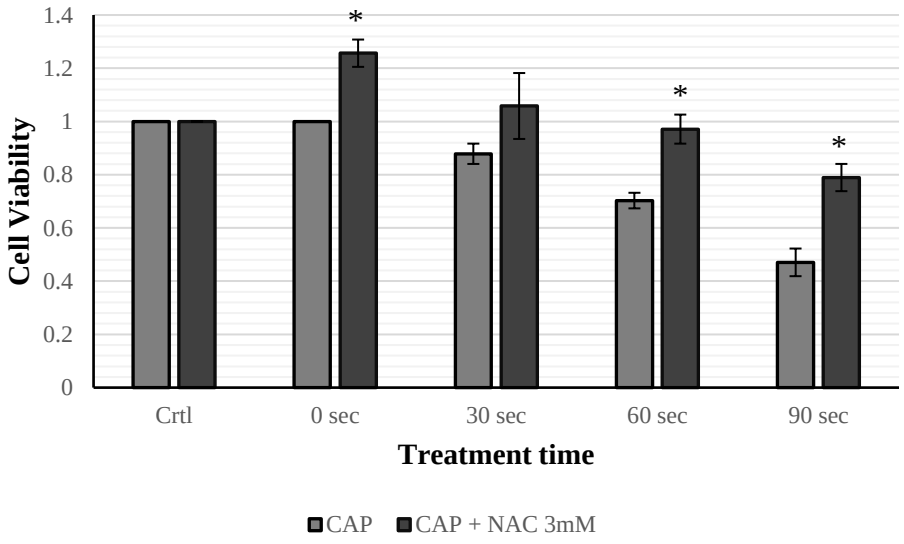

Figure 6: MTT assay 24h after combined treatment with CAP and NAC. *C6 glioma cells were incubated with CAP as described in Section 3.2.3. Fresh medium containing 3mM of NAC was added directly after CAP treatment. The graph is based on the mean value of three to four samples and has been normalized to the control. The asterisk indicates statistical significance compared to the corresponding sample treated with CAP alone.*

4.2.3 ALDH inhibition significantly enhances the effect of CAP at longer treatment times

To address the role of ALDH1 in CAP-induced treatment effects, the experiments were repeated in the presence of the ALDH inhibitor DSF. The sample only treated with DSF, as well as the samples treated additionally with CAP for 30 and 60 sec did not show any changes in cell viability. However, a significant decrease by the addition of DSF was found for the longest treatment period of 90 sec.

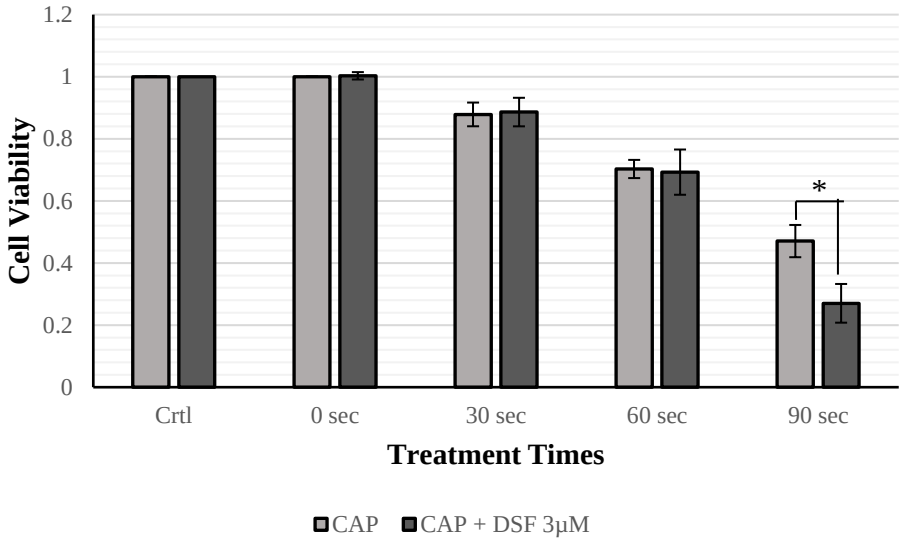

Figure 7: Cell viability after CAP treatment in combination with ALDH inhibition. *C6 glioma cells were incubated with CAP as described in Section 3.2.3. An ALDH inhibitor (3 µM DSF) was added both, 1h before CAP treatment and again directly after (now dissolved in fresh medium). The graph is based on the mean value of three to four samples and has been normalized to the control. The asterisk indicates statistical significance compared to the corresponding sample treated with CAP alone.*

4.2.4 Cell viability after radiation therapy

To assess the toxicity of different dosages of IR on C6 cells, viability assays have been performed. Whereas no alteration in cell viability was observed 24 h after IR, the MTT assay conducted after 48 h showed a decrease in cell viability with increasing IR dosages. Experimental irradiation resulted in cell reduction lower than 80 % at 6, 8 and 10 Gy after 48 h. Therefore, subeffective dosages of 2 and 4 Gy were chosen for combined treatment experiments.

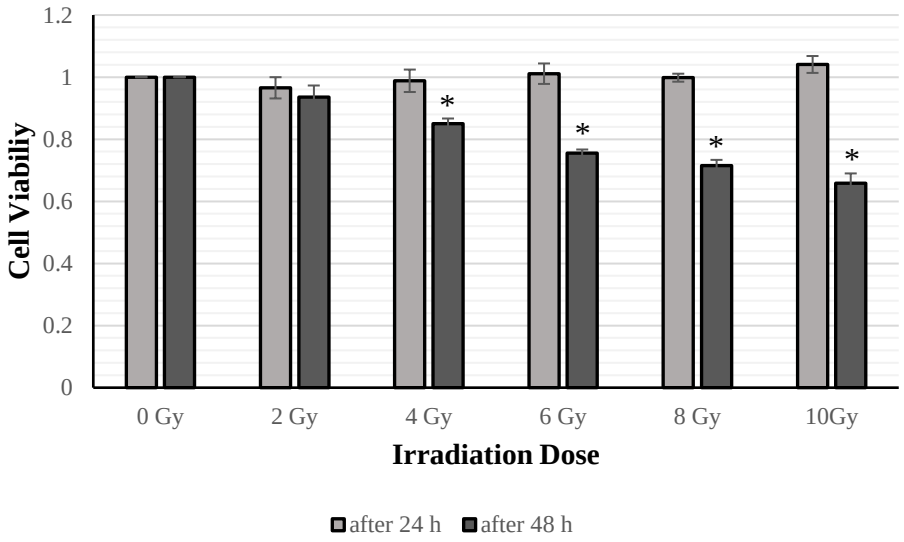

Figure 8: Cell Viability of C6 cells 24 h and 48 h after IR. *C6 glioma cells were treated with different dosages of IR in a 40mm culture dish with medium. MTT assays were performed 24 h and 48 h after the treatment. The graph is based on the mean value of three samples and has been normalized to the control. The asterisk indicates statistical significance compared to the untreated control.*

4.2.5 Cell viability after combined treatment with CAP and IR

Once the subeffective doses were determined, combined therapy experiments with CAP (30 sec and 60 sec) followed by IR (2 Gy and 4 Gy) were performed 24 h and 48 h after completion of treatment. For both measurement intervals, samples receiving combined therapy showed a reduction in cell viability compared to either treatment alone. In samples treated with CAP for 60 sec prior to IR therapy the response exceeded the additive effects of CAP and IR.

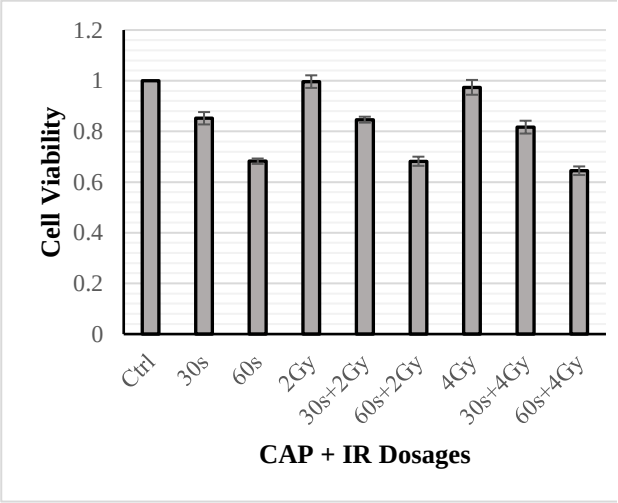

(A) 24 h after treatment

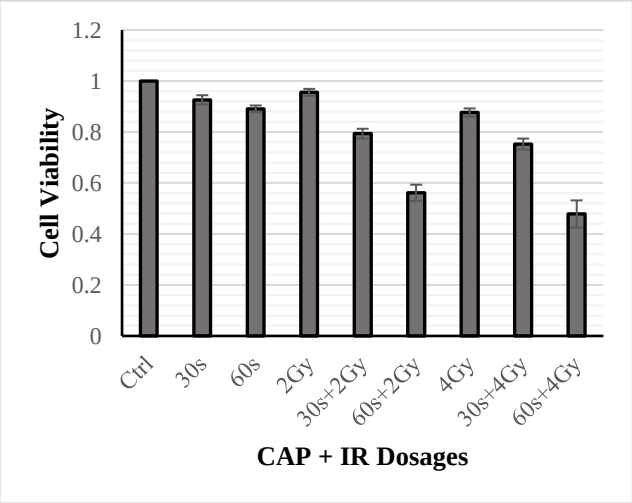

(B) 48 h after treatment

Figure 9: Cell Viability after combined treatment with CAP and IR. *C6 glioma cells were first incubated with CAP as described in Section 3.2.3. After immediate addition of fresh medium and an incubation period of 12 h, IR was performed. MTT assays were conducted **24 h (A)** and **48 h (B)** after completion of the combined treatment. The graph is based on the mean value of three samples and has been normalized to the control.*

4.3 ALDH1 expression in C6 glioma cells

4.3.1 CAP and ALDH inhibition have no influence on ALDH1 expression in C6 glioma cells

As mentioned above, ALDH1, as well as the subtypes ALDH1A1 and ALDH1A3 are potential cancer stem cell markers. The enzymes are stably expressed in C6 cells. Lysis for Western Blot analysis was performed 24h after treatment to assess the peak change in expression of ALDH1. CAP alone or in combination with the ALDH inhibitor DSF did not lead to altered expression levels of ALDH1A1 or ALDH1A3.

1

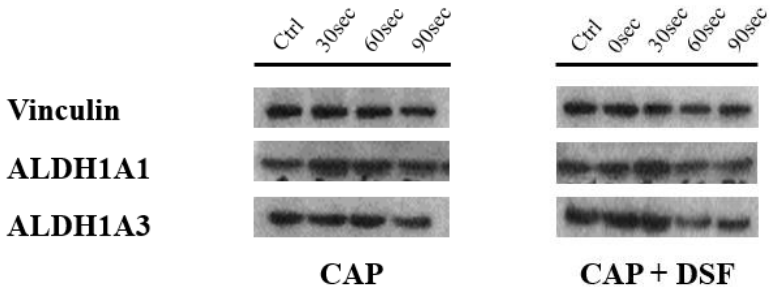

2

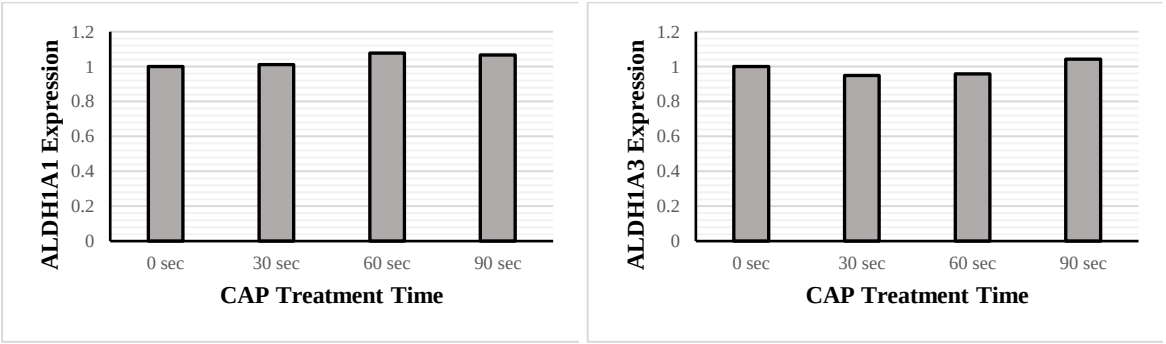

A **B**

3

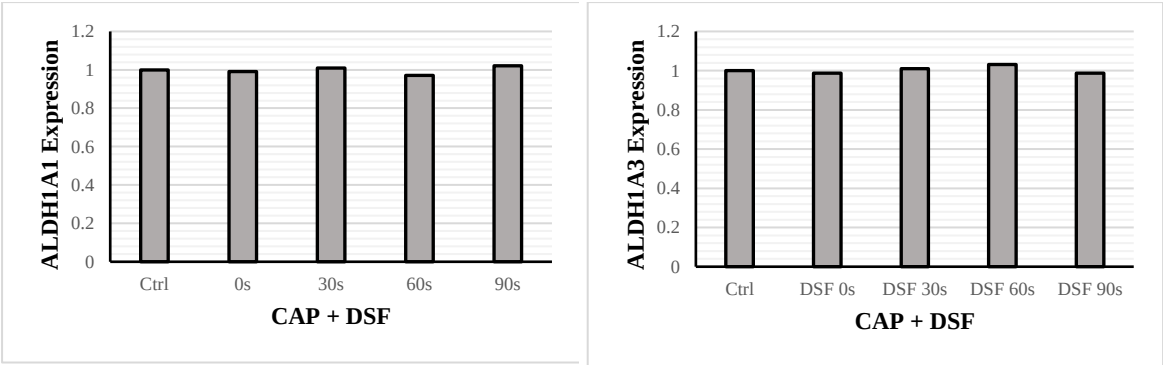

A **B**

Figure 10: ALDH1 expression in C6 cells after CAP alone and in combination with DSF. *Immunoblot analysis shows the protein expression of ALDH1A1 and ALDH1A3 which are not modified by CAP alone or in combination with DSF. Protein extraction was performed 24 h after treatment. The same protein weight (25 µg) was loaded in each lane. A scan of the original Western Blots is presented as* ***(1)****. The graphs* ***(2)*** *and* ***(3)*** *are rearranged out of the respective blot. Relative quantification analysis and normalization to the vinculin control was performed after measuring pixel density with ImageJ.*

4.3.2 Addition of NAC does not change ALDH1 expression in C6 cells

As previously described, NAC has been used to further address the role of ROS in C6 cells. In addition to the measurement of cell viability, after the described experiments, proteins were extracted by cell lysis and then purified to investigate the effect of ROS Scavenging on ALDH expression. Western Blot analysis did show no alteration of protein levels after treatment with CAP in combination with NAC.

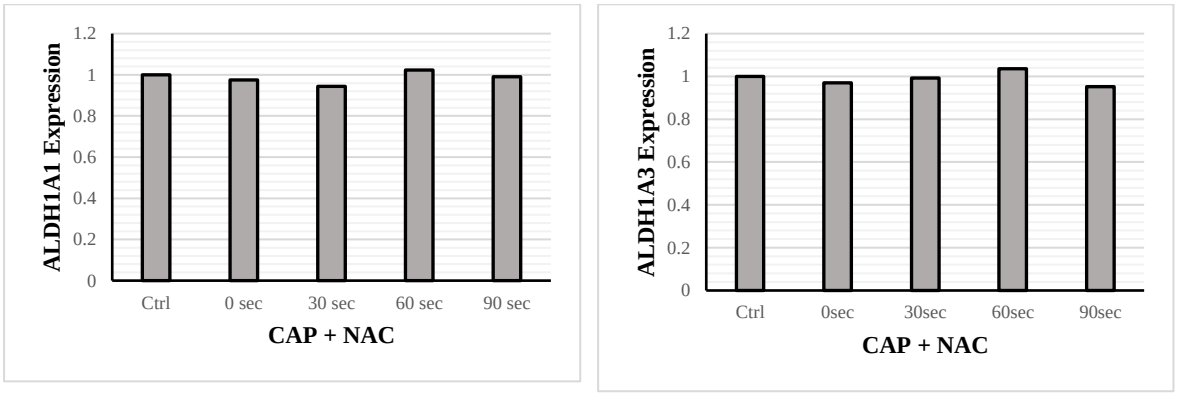

A **B**

Figure 11: ALDH1 expression in C6 cells after CAP treatment in combination with a ROS Scavenger. *Immunoblot analysis shows the protein expression of ALDH1A1 (**A**) and ALDH1A3 (**B**) which are not modified by CAP combined with the ROS Scavenger NAC. Protein extraction was performed 24 h after treatment. The same protein weight (25 µg) was loaded in each lane. For the relative quantification of the data and generation of the diagram, the same procedure was followed as described for Figure 10.*

4.3.3 IR and combination with CAP do not alter ALDH1 expression

To investigate the cause of sensitization of C6 cells to IR after CAP treatment more closely, protein was likewise extracted after IR experiments. As after sole CAP treatment, no changes in ALDH1A1 and ALDH1A3 protein expression were detected after IR alone as well as in combination with previous CAP treatment.

1

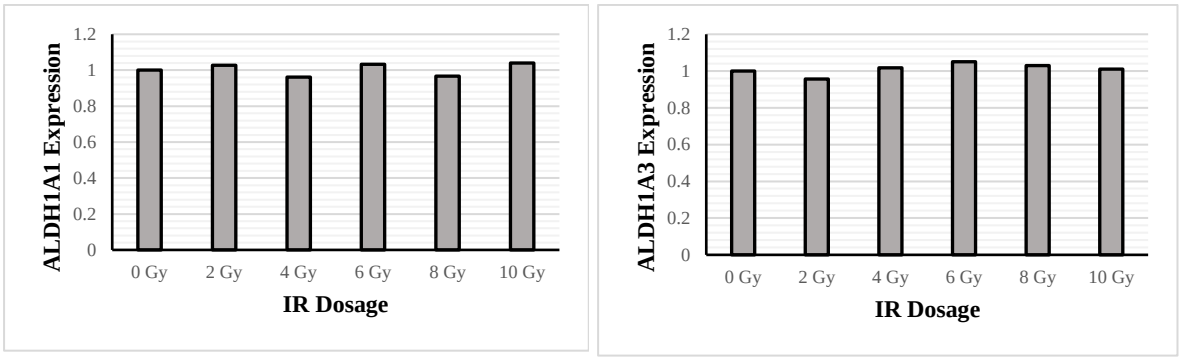

A **B**

2

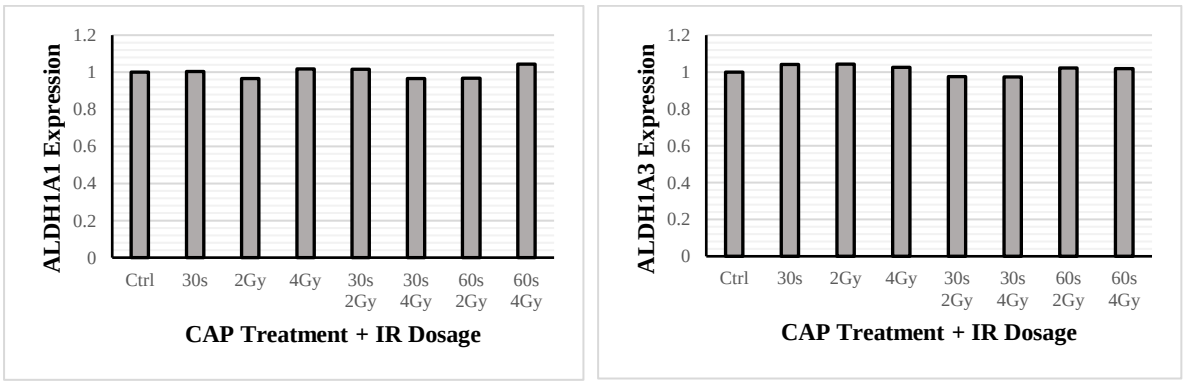

A **B**

Figure 12: ALDH1 expression in C6 cells after CAP treatment in combination with a ROS Scavenger. *Immunoblot analysis shows the protein expression of ALDH1A1 (**A**) and ALDH1A3 (**B**) which are not modified by IR alone **(1)** or with prior CAP treatment **(2)**. Protein extraction was performed 24 h after treatment. The same protein weight (25 µg) was loaded in each lane. For the relative quantification of the data and generation of the diagram, the same procedure was followed as described for Figure 10.*

4.4 Immunofluorescence visualizes ALDH1 expression in C6 cells and no alteration after Treatment with CAP, NAC and DSF.

In addition to immunoblotting, indirect immunofluorescence was performed to visualize the expression and localization of ALDH1A1/1A3. Nuclei were counterstained with DAPI. In C6 glioma cells, ubiquitous speckled cytoplasmic expression of ALDH1A1 and ALDH1A3 was detected. In line with the results obtained by immunoblotting, treatment with CAP alone as well as in combination with NAC or DSF did not modify ALDH1A1/1A3 staining intensity.

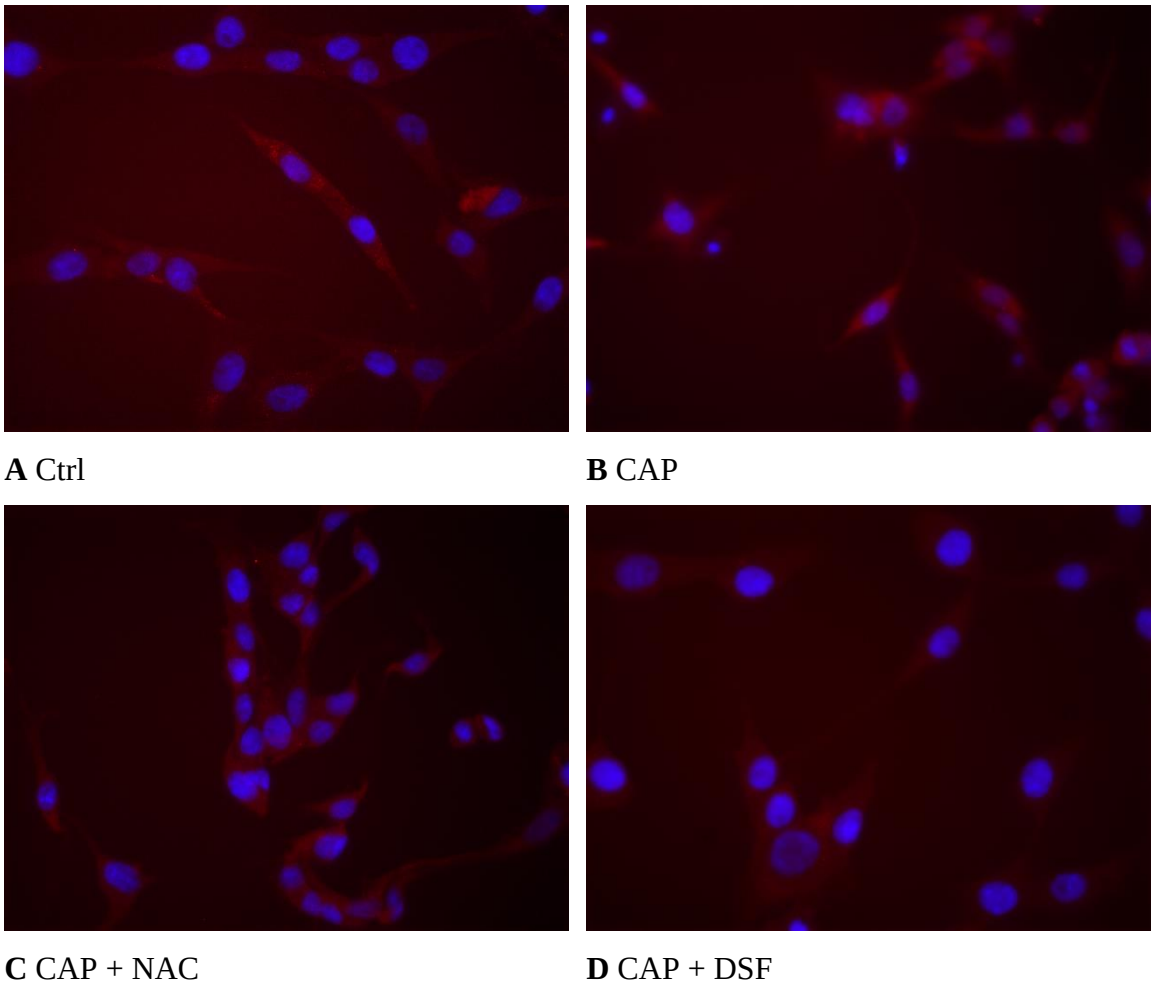

Figure 13: Immunofluorescence ALDH1A1 staining. *(Primary ALDH1A1 antibody dilution: 1:500. Magnification: 40x.) Immunofluorescence images of glioblastoma C6 cells are displayed for the following variables: untreated control **(A)**, 60 s CAP alone **(B)**, and in combination with NAC **(C)** and DSF **(D)**, respectively. Cells were fixated on the chamber slide 24 h after treatment. Cells expressing ALDH1A1 are shown in red and nuclei in blue.*

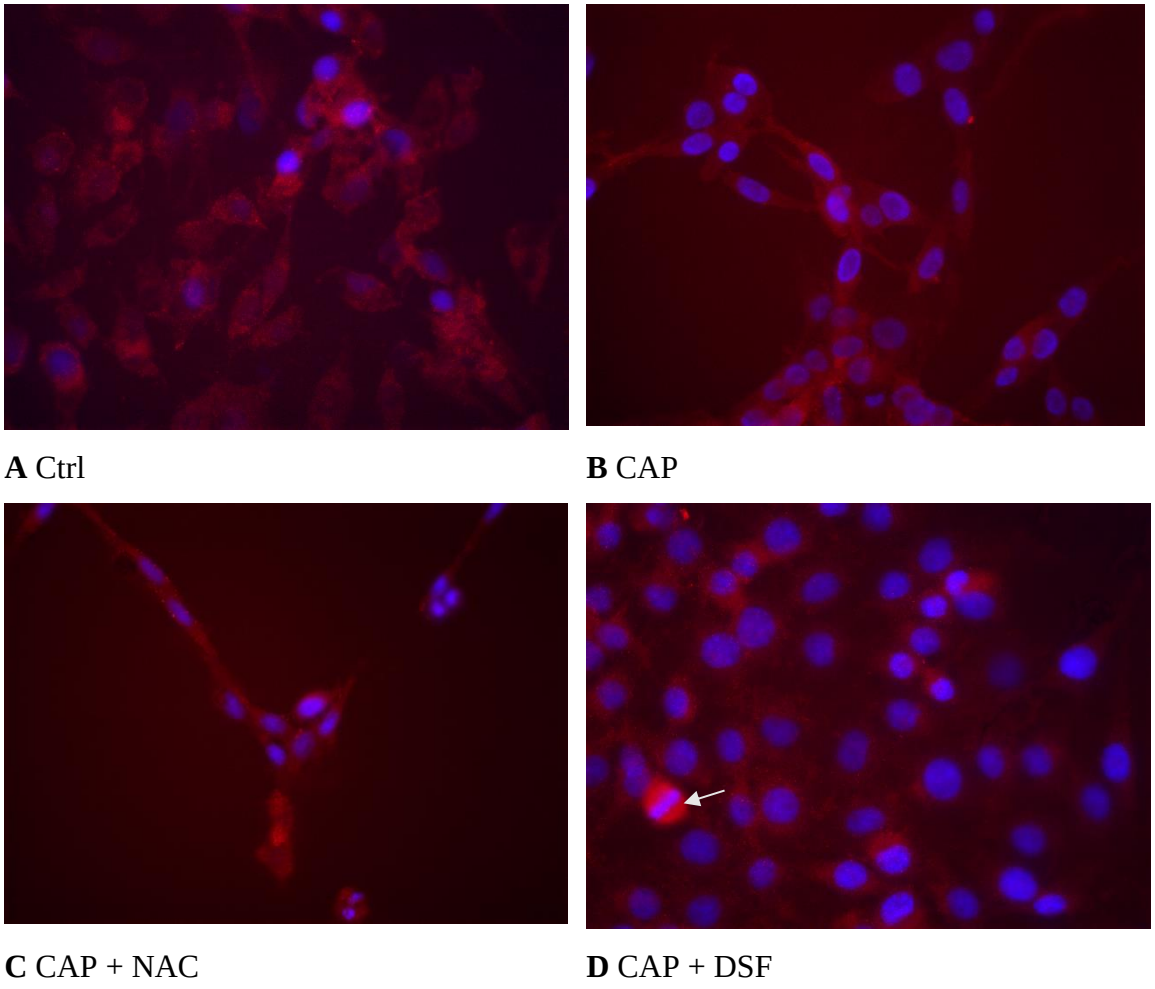

A Ctrl **B** CAP

C CAP + NAC **D** CAP + DSF

Figure 14: Immunofluorescence ALDH1A3 staining. *(Primary ALDH1A3 antibody dilution: 1:500. Magnification: 40x.) Immunofluorescence images of glioblastoma C6 cells are displayed analogously to Fig. 13. Cells were fixated on the chamber slide 24 h after treatment. Cells expressing ALDH1A3 are shown in red and nuclei in blue. The white arrow indicates a mitotic cell.*

4.5 Enzymatic ALDH Activity after CAP treatment

Enzymatic ALDH activity in C6 cells following CAP treatment was measured using Aldefluor assay. Analysis of the results revealed a decreasing enzymatic ALDH activity level with increasing treatment times. While an enzymatic ALDH activity of 22.0 % was observed in the untreated control, the sample treated with CAP for 90 sec showed an activity level of only 5.21 %.

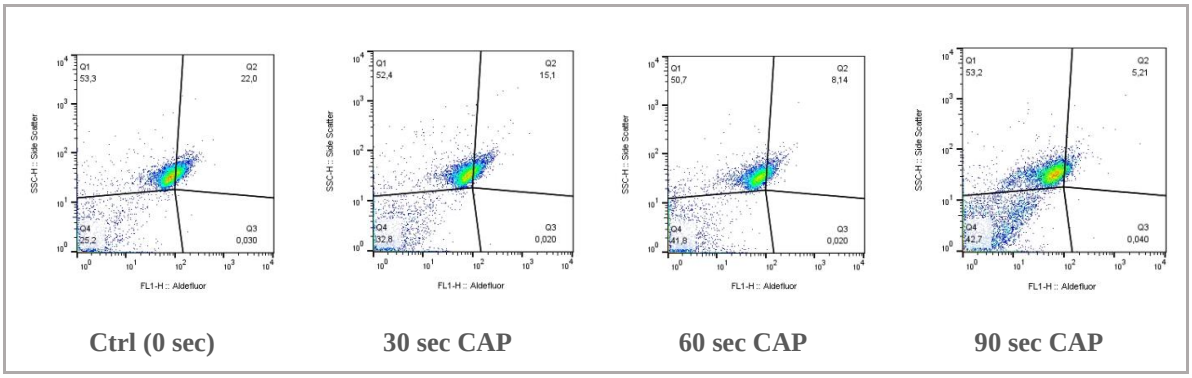

Figure 15: Aldefluor Assay after CAP treatment. *ALDH activity in C6 cells was quantified using Aldefluor Assay and FACS analysis. All samples were calibrated with a negative control inhibited with DEAB. Treatment with CAP was performed as described in Section 3.2.3.*

5 Discussion

GBM is one of the most aggressive tumor entities in humans and the most common primary brain tumor in adults. Despite intensive research in the past years, the prognosis remains very poor due to its invasiveness and inevitable recurrence. An efficient therapy is still lacking, as the underlying molecular mechanisms are far from being understood.

ALDH isozymes have been widely accepted as markers for CSC. Furthermore, initial results suggest that overexpression of ALDH in GBM is associated with resistance to therapy. The effective application of CAP to various tumor cells has recently raised hopes that CAP could be an interesting new therapeutic approach in cancer treatment. Moreover, recent studies demonstrated that CAP had been effective on glioma cells and was able to restore chemosensitivity in GBM cells. In addition, first in vivo experiments showed a significant reduction in tumor volume of different tumor entities after treatment with CAP.

Current data indicate that oxidative stress is a relevant, if not the most important, component of the therapeutic effects induced by CAP as well as IR. In addition, preliminary results from other plasma research attribute a considerable role to LPO and the accumulation of reactive aldehydes. This project investigated if these processes are interrupted by ALDH1 and if the inhibition of ALDH leads to elevated treatment effects of CAP, IR, and combined therapy.

Hereafter, the results of this project will be discussed in the context of recent studies.

5.1 CAP represents a new potential therapeutic approach for the combined treatment of GBM

In recent years, CAP has been widely discussed as a new potential therapeutic approach for the treatment of various tumor entities. CAP treatment increases intracellular ROS levels, thereby augmenting lipid peroxidation (LPO), inducing DNA double-strand breaks, and activating p53-mediated apoptosis (Choi et al., 2017; Yan et al., 2011).

In line with this, a significant decrease in cell viability in C6 cells after CAP treatment was observed in this study. The detected growth inhibition increased with the duration of treatment. Combined treatment with sub-effective dosages of CAP and IR led to a cell reduction that was more effective than the maximum tested dosages of either treatment alone, indicating that CAP can enhance the efficacy of radiotherapy and might be able to reduce radio resistance. Taken together with the previously demonstrated increased sensitivity of GBM cells to TMZ (Koritzer et al., 2013), this could lead to a significantly improved response to the existing standard therapy when preceded by CAP treatment.

The mentioned impact of the combined therapy of CAP and IR was only visible 48 hours after IR treatment, while after 24 hours no effect had occurred. The same is true for sole IR therapy. This is consistent with the typically protracted response of solid tumors to IR triggered by DNA damage and resulting mitotic failure. Only after several attempted divisions, enough genetic damage has accumulated to trigger programmed cell death (Sia et al., 2020).

Recent publications demonstrated that in the effects induced by CAP, cell cycle arrest was shown to play a prominent role. In different cancer cell models CAP treatment causes cell cycle arrest in the G2-Phase for at least 72 hrs, but with some of the cells already starting to recover between 24 to 48 hrs after treatment (Koritzer et al., 2013; Yan et al., 2010). Volotskova et al. observed a significant decrease of cells in S-Phase immediately and 4 hrs after CAP treatment which had already converted after 24 hrs (Volotskova et al., 2012). Taking into consideration the estimated doubling time for C6 cells of 24-28 h (Kuduvalli et al., 2019), these findings could explain the again increased cell viability shown in Figure 10 (B) compared to Figure 10 (A) of this study. Since IR was performed 12 hrs after CAP treatment, 60 hrs elapsed between the initial CAP treatment and the evaluation by MTT assay in the experiment shown in Figure 10 (B).

For a certain number of C6 cells, this time span may be sufficient to recover from cell cycle arrest and start proliferating again. This draws a line to the complexity of intracellular events following CAP treatment, only a fraction of which have been understood to date. In the future, it will be important to collect data on the long-term effects of CAP, as well as to investigate further treatment options such as repeated treatment cycles, thereby establishing the basis for an optimal CAP treatment setting for in vivo experiments.

An obstacle for in vivo studies and clinical trials will certainly be the penetration depth of CAP, which is described as approximately 50 mm (Partecke et al., 2012). On the other hand, Bauer et al. concluded that the ROS generated by CAP mainly act as a trigger factor to induce further intracellular ROS production and that it may be possible to reach interior parts of a solid tumor by maintaining these harmful mechanisms (Bauer et al., 2019). This in turn is raising hope that CAP could be successfully applied in the clinical setting and could also explain the observed reduced tumor volume in several studies in vivo.

In summary, the cell viability data clearly demonstrates not only that CAP can dramatically reduce the number of viable C6 GBM cells, but also that the cytotoxicity of IR is enhanced in the presence of CAP. These results provide compelling evidence for the important role of CAP in suppressing cancer cells both alone as well as in combination with IR and highlight the need for further investigation into the mechanisms involved.

5.2 Unveiling the role of ROS can contribute to a better understanding of tumors

As mentioned above, ROS production is not only thought to play a central role in CAP-induced treatment effects but it has also been used for some time as an important component of established cancer therapies such as chemotherapy and IR (Choi et al., 2017; Perillo et al., 2020).

These ideas are reflected in the results of this project, as the addition of ROS scavengers blocked the effect of CAP. Strikingly, with increasing treatment duration, the entire effect on cell viability could no longer be intercepted by the ROS scavenger.

This may suggest that other species or effects are involved in the action of CAP that cannot be counteracted by NAC. Another explanation could be that the dose of NAC used may have been out of the optimal range of effect despite appropriate preliminary testing.

Nevertheless, it can be concluded that the therapeutic effect of CAP is to some extent due to oxidative stress. Correspondingly, publications of recent years leave no doubt that ROS are responsible for at least a considerable part of the effects caused by CAP (Liu et al., 2017; Yan et al., 2015). Yet, since CAP can be adjusted individually by the setting of the device used, this extent will most likely vary between different devices.

Furthermore, the often discussed dual and opposing effects of ROS in cancer development and control should be mentioned in this context. As described above, tumor cells are more prone to accumulate ROS than normal cells and increasing ROS in tumor cells or targeting the redox system can therefore selectively eliminate tumor cells without relevantly harming normal cells. On the other hand, it is known that tumor cells require slightly elevated ROS levels to maintain their altered metabolism. It is therefore of utmost importance to further investigate the underlying intracellular pathways to overcome the redox capacity of cancer cells while causing as little damage as possible to normal non-neoplastic cells. Certainly, further experiments and close interdisciplinary collaboration between physics, cancer research, and medicine are necessary to generate the optimal CAP gas mixture for targeting the respective tumor entity.

5.3 ALDH1 and therapy resistance

In certain malignant tumors, cells with high ALDH activity have been detected, which simultaneously exhibit low ROS levels. Other studies have illustrated the protection of CSCs from ROS by ALDH. However, it is unclear how ALDH expression is related to or mediates therapy resistance.

Preliminary results and the known detoxifying functions of ALDH suggest that these cells have higher antioxidant potential. (Rasper et al., 2010; Schäfer et al., 2012). Several research groups have focused on the ALDH1 subfamily and especially the two enzymes ALDH1A1 and ALDH1A3, as they seem to be related to CSC properties and therapy resistance. There's evidence of an association of ALDH1A1/ALDH1A3 expression with aggressiveness and poor clinical outcome in several tumor entities (Chen et al., 2009; Liu et al., 2012; Wang et al., 2017). Furthermore, enhanced ALDH1A1 and ALDH1A3 expression was found in patient samples of recurrent GBM and may be related to the increased resistance to therapy of recurrent tumors (Schäfer et al., 2012; Wu et al., 2020).

As shown in Figure 8 in the conducted experiment using CAP on C6 glioma the ALDH inhibitor DSF enhanced the effects on cell viability at longer treatment times.

This enhancement of effects suggests that glioma cells benefit from some protection by ALDH against the mechanisms induced by CAP. Considering the effect of NAC mentioned in 5.2. together this can be explained best by the ability of ALDH enzymes to compensate for the cell-damaging effect of ROS and reactive aldehydes (Xu et al., 2015). In addition, DSF itself has been attributed an anti-cancer capacity in other tumor entities, as it is able to enhance the cytotoxicity of radiotherapy as well as of other anti-cancer drugs. (Liu et al., 2016; Rae et al., 2013). Certainly, the non-specific inhibition by DSF should be mentioned here as a limiting factor. The amplification of CAP-induced effects by DSF cannot be clearly attributed to the activity of ALDH1A1/1A3 but could also be due to other ALDH isoenzymes. This long-standing lack of selectivity of available ALDH isoenzyme antagonists has recently been addressed by the introduction of several molecules with specific inhibitory activity against ALDH1A1 and ALDH1A3 (Condello et al., 2015; Li et al., 2021). However, with limited data available for the newly introduced specific inhibitors, adverse consequences such as pharmacological side effects or residual nonspecific inhibitory activity cannot be ruled out, and stable knockout of ALDH1A1/1A3 therefore

remains the primary method for more specific investigation of the effects of ALDH1A1/1A3 on distinct GBM properties. Due to resource restrictions, genetic knock-out was not performed within this project.

In contrast to the significant decrease of ALDH activity following CAP treatment, shown in Figure 15, there was no alteration of ALDH1A1 or ALDH1A3 protein levels observed in this study. Hence, it must be assumed that the reduced enzyme activity is not caused by changes in protein level.

Enzyme activity is influenced by a number of external factors such as temperature, pH, and, most importantly, substrate concentration. Initially, an increase in substrate concentration leads to an increased rate of a enzyme-catalyzed reaction. When the enzyme molecules are saturated with substrate, this increase in reaction rate flattens out. The Michaelis-Menten equation describes this hyperbolic increase of enzyme activity as substrate concentration raises until the maximum is reached (Michaelis & Menten, 1913). Conversely, this implies that while at low substrate concentrations the binding site is occupied more efficiently, an ever-increasing amount of substrate is required as occupancy progresses. Therefore high concentrations can then even lead to so-called substrate inhibition, i.e. the respective enzyme is inhibited by an increased concentration of its own substrate (Bisswanger, 2014).

Deriving from this, one can conclude that a cascade of extrinsic and intrinsic oxidative stress triggered by CAP may lead to an excess of lipid peroxidation, consequent production of reactive aldehydes, and thus, by substrate inhibition, the measured reduction of ALDH activity.

This conclusion is supported by findings of increased lipid peroxidation levels in different tumor entities after CAP treatment (Alimohammadi et al., 2020; Yan et al., 2011). In addition, Bauer et al. demonstrated that the reactive oxygen species derived from CAP lead to an auto-amplificatory generation of secondary ROS by inactivation of key components of the redox system in the tumor cells and that these mechanisms are sustained over a comparatively long period of up to several days. In this context, lipid peroxidation triggered the mitochondrial pathway of apoptosis only when intracellular glutathione levels were diminished (Bauer et al., 2019). In line with this, a decreased antioxidant activity in U937 lymphoma cells was reported following CAP treatment (Kaushik et al., 2014).

This contradicts the usual increase of glutathione by ROS-sensitive transcription factors and suggests that the interactions between CAP, ROS, and the antioxidant capacity of tumor cells are highly complex and most likely influence and reinforce each other. To corroborate the data of this study, further experiments should be performed to detect ROS concentration as well as lipid peroxidation or accumulation of aldehydes following CAP treatment.

In the present study, stable expression of ALDH1A1 and ALDH1A3 in C6 glioma cells was detected by Western blot analysis as well as immunofluorescence staining. Although the involvement of ALDH in the effects induced by CAP can be assumed based on the results on ALDH enzyme activity and after ALDH inhibition, surprisingly, no change in protein levels of ALDH1A1 and ALDH1A3 occurred after treatment with CAP.

In consequence, it must be considered that the protection mediated by ALDH in C6 cells is not regulated at the transcriptional level. Indeed, an increase in both ALDH1A1 and ALDH1A3 levels has previously been observed in association with acquired resistance after standard chemo - and radiotherapy. So far, no cases of resistance development after CAP treatment have been reported.

Therefore, it may be possible that although ALDH mediates baseline intrinsic resistance through its antioxidant capacity, there is no change in protein levels after CAP treatment and thus no change in the resistance status. Yet, the plausibility of this explanatory approach is significantly weakened by the fact that in the present project there were no changes in Western blot analysis even following IR.

Another possible explanation could be that the timing of cell lysis was not optimal. Wu et al. have recently described that ALDH1A3 levels in several established glioma cell lines are reduced immediately after termination of TMZ therapy but subsequently increase significantly with a delay of several days (Wu et al., 2020). It, therefore, stands to reason that some changes in protein expression would also be seen in this project if cell lysates for Western blot analysis were prepared at different time points.

All in all, the results of this work clearly demonstrate that ALDH is involved in the treatment effects of CAP and that C6 glioma cells benefit from the antioxidant protection of ALDH. This indicates ALDH as a useful therapeutic target, especially in tumors deriving from tissues that usually don’t express ALDH at high levels.

Although C6 cells are considered the gold standard for in vitro GBM research (Giakoumettis et al., 2018), it may be worthwhile to perform experiments with other established GBM cell lines as well as in a tumor sphere model to obtain more comprehensive data from a tumor model that is as similar as possible to the heterogeneity and microenvironment of GBM.

6 Summary

GBM is the most common and deadly of all brain tumors in adulthood. Treatment resistance and inevitable relapse remain the main obstacle to the improvement of prognosis and survival time. Preliminary results suggest that overexpression of ALDH in GBM is associated with therapy resistance and ALDH may serve as a prognostic marker for GBM. CAP is not only discussed as a new effective therapeutic approach, especially for its selectivity for cancer cells but as well has been able to restore chemosensitivity in GBM cells. This work aimed to better understand the role of ALDH1 in mediating therapy resistance and the underlying molecular mechanisms of CAP effects in cancer treatment.

C6 glioma cells were treated with CAP, either alone or in combination with conventional IR, and additionally in the presence of a ROS scavenger and an ALDH inhibitor. The effects on cell viability and ALDH1 expression and activity were assessed using standard protocols such as MTT assay, Western blot, and Aldefluor assay.

Progressive growth inhibition in C6 cells was observed with increasing CAP treatment times. Combined treatment at sub-effective doses of CAP and IR led to a significant cell reduction that was more effective than the maximal tested dosages of either treatment alone. By scavenging ROS, the effect of CAP, both alone and in combination with IR, was attenuated. ALDH inhibitors enhanced the effects on cell viability at longer treatment times. Although a significant decrease in ALDH activity was detected following CAP treatment, no alteration of ALDH1 protein levels was observed.

The results clearly indicate that CAP can improve the efficiency of standard radiotherapy, making it a promising candidate for the therapy of GBM. In addition, they demonstrate the role of ALDH in the mediated treatment effects, as its inhibition leads to an accentuation of these effects and the enzyme activity data show that ALDH is involved in the processing of the induced intracellular stress. CAP as part of a multimodal adjuvant combination treatment can likely contribute to relevant success against GBM as well as other tumor entities. Intensive interdisciplinary collaboration will be necessary to finally make progress in the ongoing battle against treatment resistance and the fatal outcome of GBM.

Acknowledgment

Über die Jahre, die ich an diesem Projekt gearbeitet habe, haben mich so viele Freunde und Kollegen unterstützt, dass ich leider nicht alle namentlich erwähnen kann. Daher möchte ich mich vorab bei all denjenigen bedanken, die sich regelmäßig nach dem Stand meiner Doktorarbeit erkundigt haben und immer ein offenes Ohr für mich hatten.

Besonderer Dank gebührt meinem Doktorvater Prof. Jürgen Schlegel, der es mir ermöglicht hat in familiärer Atmosphäre in die Welt der experimentellen Forschung einzusteigen. Besonders beeindruckt hat mich, dass du nicht nur in den wöchentlichen Meetings jedes Projekt der vielen Mitglieder der Arbeitsgruppe ausführlich besprichst, sondern auch darüber hinaus immer niederschwellig für Fragen zur Verfügung stehst.

Ohne die vielen Mitglieder der AG Schlegel (auch hier kann ich leider nicht alle namentlich nennen) wäre meine Zeit in der Neuropathologie sicherlich nur halb so schön gewesen. Allen voran möchte ich Fritzi und Laura danken, die in dieser Zeit gewissermaßen die Konstante und das Herz der Arbeitsgruppe waren und uns jederzeit mit Rat und Tat zur Seite standen. Besonders dankbar bin ich außerdem für die tatkräftige Hilfe von Sandra und Christian bei der Durchführung der Experimente.

Nicht zuletzt möchte ich mich bei meiner Familie und meinem Partner Arturo bedanken. Euer stetiger Zuspruch, eure Geduld und vor allem euer Interesse und Verständnis für ein für euch „fachfremdes“ Thema, haben mich motiviert, am Ball zu bleiben und diese Arbeit fertig zu stellen. Danke, dass ich immer auf eure Unterstützung zählen kann.

References

Alimohammadi, M., Golpur, M., Sohbatzadeh, F., Hadavi, S., Bekeschus, S., Niaki, H. A., Valadan, R., & Rafiei, A. (2020, Jul 8). Cold Atmospheric Plasma Is a Potent Tool to Improve Chemotherapy in Melanoma In Vitro and In Vivo. *Biomolecules, 10*(7), 1011. https://doi.org/10.3390/biom10071011

Ayliffe, G. (2000, Aug). Decontamination of minimally invasive surgical endoscopes and accessories. *J Hosp Infect, 45*(4), 263-277. https://doi.org/10.1053/jhin.2000.0767

Barrera, G., Pizzimenti, S., & Dianzani, M. U. (2008, Feb-Apr). Lipid peroxidation: control of cell proliferation, cell differentiation and cell death. *Mol Aspects Med, 29*(1-2), 1-8. https://doi.org/10.1016/j.mam.2007.09.012

Bauer, G., Sersenová, D., Graves, D. B., & Machala, Z. (2019, Oct 2). Cold Atmospheric Plasma and Plasma-Activated Medium Trigger RONS-Based Tumor Cell Apoptosis. *Sci Rep, 9*(1), 14210. https://doi.org/10.1038/s41598-019-50291-0

Bell, R. G., & Smith, H. W. (1949, Mar). Preliminary report on clinical trials of antabuse. *Can Med Assoc J, 60*(3), 286-288.

Bisswanger, H. (2014). Enzyme Assays. *Perspectives in Science, 1*(1–6), 41-55. https://doi.org/10.1016/j.pisc.2014.02.005

Bonnet, D., & Dick, J. E. (1997, Jul). Human acute myeloid leukemia is organized as a hierarchy that originates from a primitive hematopoietic cell. *Nat Med, 3*(7), 730-737. https://doi.org/10.1038/nm0797-730

Brat, D. J., Aldape, K., Colman, H., Figrarella-Branger, D., Fuller, G. N., Giannini, C., Holland, E. C., Jenkins, R. B., Kleinschmidt-DeMasters, B., Komori, T., Kros, J. M., Louis, D. N., McLean, C., Perry, A., Reifenberger, G., Sarkar, C., Stupp, R., van den Bent, M. J., von Deimling, A., & Weller, M. (2020, Mar). cIMPACT-NOW update 5: recommended grading criteria and terminologies for IDH-mutant astrocytomas. *Acta Neuropathol, 139*(3), 603-608. https://doi.org/10.1007/s00401-020-02127-9

Chen, J., Li, Y., Yu, T. S., McKay, R. M., Burns, D. K., Kernie, S. G., & Parada, L. F. (2012, Aug 23). A restricted cell population propagates glioblastoma growth after chemotherapy. *Nature, 488*(7412), 522-526. https://doi.org/10.1038/nature11287

Chen, Y. C., Chen, Y. W., Hsu, H. S., Tseng, L. M., Huang, P. I., Lu, K. H., Chen, D. T., Tai, L. K., Yung, M. C., Chang, S. C., Ku, H. H., Chiou, S. H., & Lo, W. L. (2009, Jul 31). Aldehyde dehydrogenase 1 is a putative marker for cancer stem cells in head and neck squamous cancer. *Biochem Biophys Res Commun, 385*(3), 307-313. https://doi.org/10.1016/j.bbrc.2009.05.048

Choi, J. S., Kim, J., Hong, Y. J., Bae, W. Y., Choi, E. H., Jeong, J. W., & Park, H. K. (2017, May 1). Evaluation of non-thermal plasma-induced anticancer effects on human colon cancer cells. *Biomed Opt Express, 8*(5), 2649-2659. https://doi.org/10.1364/BOE.8.002649

Condello, S., Morgan, C. A., Nagdas, S., Cao, L., Turek, J., Hurley, T. D., & Matei, D. (2015, Apr 30). β-Catenin-regulated ALDH1A1 is a target in ovarian cancer spheroids. *Oncogene, 34*(18), 2297-2308. https://doi.org/10.1038/onc.2014.178

Ellis, H. P., Greenslade, M., Powell, B., Spiteri, I., Sottoriva, A., & Kurian, K. M. (2015). Current Challenges in Glioblastoma: Intratumour Heterogeneity, Residual Disease, and Models to Predict Disease Recurrence. *Front Oncol, 5*, 251. https://doi.org/10.3389/fonc.2015.00251

Espinosa-Diez, C., Miguel, V., Mennerich, D., Kietzmann, T., Sánchez-Pérez, P., Cadenas, S., & Lamas, S. (2015, Dec). Antioxidant responses and cellular adjustments to oxidative stress. *Redox Biol, 6*, 183-197. https://doi.org/10.1016/j.redox.2015.07.008

Fridman, G., Friedman, G., Gutsol, A., Shekhter, A. B., Vasilets, V. N., & Fridman, A. (2008). Applied Plasma Medicine. *Plasma Process. Polym. , 5*, 503-533

Giakoumettis, D., Kritis, A., & Foroglou, N. (2018, Jul-Sep). C6 cell line: the gold standard in glioma research. *Hippokratia, 22*(3), 105-112. PMCID: 6801124

Giese, A., & Westphal, M. (2001, Apr). Treatment of malignant glioma: a problem beyond the margins of resection. *J Cancer Res Clin Oncol, 127*(4), 217-225. https://doi.org/10.1007/s004320000188

Gupta, S. C., Hevia, D., Patchva, S., Park, B., Koh, W., & Aggarwal, B. B. (2012, Jun 1). Upsides and downsides of reactive oxygen species for cancer: the roles of reactive oxygen species in tumorigenesis, prevention, and therapy. *Antioxid Redox Signal, 16*(11), 1295-1322. https://doi.org/10.1089/ars.2011.4414

Hegi, M. E., Liu, L., Herman, J. G., Stupp, R., Wick, W., Weller, M., Mehta, M. P., & Gilbert, M. R. (2008, Sep 1). Correlation of O6-methylguanine methyltransferase (MGMT) promoter methylation with clinical outcomes in glioblastoma and clinical strategies to modulate MGMT activity. *J Clin Oncol, 26*(25), 4189-4199. https://doi.org/10.1200/jco.2007.11.5964

Hermann, P. C., Huber, S. L., Herrler, T., Aicher, A., Ellwart, J. W., Guba, M., Bruns, C. J., & Heeschen, C. (2007, Sep 13). Distinct populations of cancer stem cells

determine tumor growth and metastatic activity in human pancreatic cancer. *Cell Stem Cell, 1*(3), 313-323. https://doi.org/10.1016/j.stem.2007.06.002

Isbary, G., Shimizu, T., Li, Y. F., Stolz, W., Thomas, H. M., Morfill, G. E., & Zimmermann, J. L. (2013, May). Cold atmospheric plasma devices for medical issues. *Expert Rev Med Devices, 10*(3), 367-377. https://doi.org/10.1586/erd.13.4

Kaushik, N., Kumar, N., Kim, C. H., Kaushik, N. K., & Choi, E. H. (2014). Dielectric Barrier Discharge Plasma Efficiently Delivers an Apoptotic Response in Human Monocytic Lymphoma. *Plasma Process Polym, 11*(12), 1175-1187. https://doi.org/10.1002/ppap.201400102

Keidar, M., Walk, R., Shashurin, A., Srinivasan, P., Sandler, A., Dasgupta, S., Ravi, R., Guerrero-Preston, R., & Trink, B. (2011, Oct 25). Cold plasma selectivity and the possibility of a paradigm shift in cancer therapy. *Br J Cancer, 105*(9), 1295-1301. https://doi.org/10.1038/bjc.2011.386

Kim, J. Y., Cho, Y., Oh, E., Lee, N., An, H., Sung, D., Cho, T. M., & Seo, J. H. (2016, Aug 28). Disulfiram targets cancer stem-like properties and the HER2/Akt signaling pathway in HER2-positive breast cancer. *Cancer Lett, 379*(1), 39-48. https://doi.org/10.1016/j.canlet.2016.05.026

Koritzer, J., Boxhammer, V., Schafer, A., Shimizu, T., Klampfl, T. G., Li, Y. F., Welz, C., Schwenk-Zieger, S., Morfill, G. E., Zimmermann, J. L., & Schlegel, J. (2013). Restoration of sensitivity in chemo-resistant glioma cells by cold atmospheric plasma. *PLoS One, 8*(5), e64498. https://doi.org/10.1371/journal.pone.0064498

Kuduvalli, S., Ramalakshmi, O., Daisy Precilla, S., & Anitha, T. (2019). Evaluation of Cell Doubling Time in C6 and Y79 Cell Lines Based on Seeding Density. *SBV Journal of Basic, Clinical and Applied Health Science*(2(4)), 146-149. https://doi.org/10.5005/jp-journals-10082-02230.

Lapointe, S., Perry, A., & Butowski, N. A. (2018, Aug 4). Primary brain tumours in adults. *Lancet, 392*(10145), 432-446. https://doi.org/10.1016/s0140-6736(18)30990-5

Li, J., Garavaglia, S., Ye, Z., Moretti, A., Belyaeva, O. V., Beiser, A., Ibrahim, M., Wilk, A., McClellan, S., Klyuyeva, A. V., Goggans, K. R., Kedishvili, N. Y., Salter, E. A., Wierzbicki, A., Migaud, M. E., Mullett, S. J., Yates, N. A., Camacho, C. J., Rizzi, M., & Sobol, R. W. (2021, Dec 21). A specific inhibitor of ALDH1A3 regulates retinoic acid biosynthesis in glioma stem cells. *Commun Biol, 4*(1), 1420. https://doi.org/10.1038/s42003-021-02949-7

Li, T., Su, Y., Mei, Y., Leng, Q., Leng, B., Liu, Z., Stass, S. A., & Jiang, F. (2010, Feb). ALDH1A1 is a marker for malignant prostate stem cells and predictor of prostate

cancer patients' outcome. *Lab Invest, 90*(2), 234-244. https://doi.org/10.1038/labinvest.2009.127

Liu, D. Y., Ren, C. P., Yuan, X. R., Zhang, L. H., Liu, J., Liu, Q., Yuan, J., Yuan, D., & Jiang, X. J. (2012, Dec). ALDH1 expression is correlated with pathologic grade and poor clinical outcome in patients with astrocytoma. *J Clin Neurosci, 19*(12), 1700-1705. https://doi.org/10.1016/j.jocn.2012.01.036

Liu, X., Wang, L., Cui, W., Yuan, X., Lin, L., Cao, Q., Wang, N., Li, Y., Guo, W., Zhang, X., Wu, C., & Yang, J. (2016, Sep 6). Targeting ALDH1A1 by disulfiram/copper complex inhibits non-small cell lung cancer recurrence driven by ALDH-positive cancer stem cells. *Oncotarget, 7*(36), 58516-58530. https://doi.org/10.18632/oncotarget.11305

Liu, Y., Tan, S., Zhang, H., Kong, X., Ding, L., Shen, J., Lan, Y., Cheng, C., Zhu, T., & Xia, W. (2017, Aug 11). Selective effects of non-thermal atmospheric plasma on triple-negative breast normal and carcinoma cells through different cell signaling pathways. *Sci Rep, 7*(1), 7980. https://doi.org/10.1038/s41598-017-08792-3

Louis, D. N., Perry, A., Reifenberger, G., von Deimling, A., Figarella-Branger, D., Cavenee, W. K., Ohgaki, H., Wiestler, O. D., Kleihues, P., & Ellison, D. W. (2016, Jun). The 2016 World Health Organization Classification of Tumors of the Central Nervous System: a summary. *Acta Neuropathol, 131*(6), 803-820. https://doi.org/10.1007/s00401-016-1545-1

Louis, D. N., Perry, A., Wesseling, P., Brat, D. J., Cree, I. A., Figarella-Branger, D., Hawkins, C., Ng, H. K., Pfister, S. M., Reifenberger, G., Soffietti, R., von Deimling, A., & Ellison, D. W. (2021, Aug 2). The 2021 WHO Classification of Tumors of the Central Nervous System: a summary. *Neuro Oncol, 23*(8), 1231-1251. https://doi.org/10.1093/neuonc/noab106

Mao, P., Joshi, K., Li, J., Kim, S. H., Li, P., Santana-Santos, L., Luthra, S., Chandran, U. R., Benos, P. V., Smith, L., Wang, M., Hu, B., Cheng, S. Y., Sobol, R. W., & Nakano, I. (2013, May 21). Mesenchymal glioma stem cells are maintained by activated glycolytic metabolism involving aldehyde dehydrogenase 1A3. *Proc Natl Acad Sci U S A, 110*(21), 8644-8649. https://doi.org/10.1073/pnas.1221478110

Marchitti, S. A., Brocker, C., Stagos, D., & Vasiliou, V. (2008, Jun). Non-P450 aldehyde oxidizing enzymes: the aldehyde dehydrogenase superfamily. *Expert Opin Drug Metab Toxicol, 4*(6), 697-720. https://doi.org/10.1517/17425255.4.6.697

Michaelis, L., & Menten, M. L. (1913). Die Kinetik der Invertinwirkung. *Biochemische Zeitschrift*(49), 333–369.

Moloney, J. N., & Cotter, T. G. (2018, Aug). ROS signalling in the biology of cancer. *Semin Cell Dev Biol, 80*, 50-64. https://doi.org/10.1016/j.semcdb.2017.05.023

Niederreither, K., Fraulob, V., Garnier, J. M., Chambon, P., & Dolle, P. (2002, Jan). Differential expression of retinoic acid-synthesizing (RALDH) enzymes during fetal development and organ differentiation in the mouse. *Mech Dev, 110*(1-2), 165-171. https://doi.org/10.1016/s0925-4773(01)00561-5

Ostrom, Q. T., Cioffi, G., Waite, K., Kruchko, C., & Barnholtz-Sloan, J. S. (2021, Oct 5). CBTRUS Statistical Report: Primary Brain and Other Central Nervous System Tumors Diagnosed in the United States in 2014-2018. *Neuro Oncol, 23*(12 Suppl 2), iii1-iii105. https://doi.org/10.1093/neuonc/noab200

Partecke, L. I., Evert, K., Haugk, J., Doering, F., Normann, L., Diedrich, S., Weiss, F. U., Evert, M., Huebner, N. O., Guenther, C., Heidecke, C. D., Kramer, A., Bussiahn, R., Weltmann, K. D., Pati, O., Bender, C., & von Bernstorff, W. (2012, Oct 15). Tissue tolerable plasma (TTP) induces apoptosis in pancreatic cancer cells in vitro and in vivo. *BMC Cancer, 12*, 473. https://doi.org/10.1186/1471-2407-12-473

Pelicano, H., Carney, D., & Huang, P. (2004, Apr). ROS stress in cancer cells and therapeutic implications. *Drug Resist Updat, 7*(2), 97-110. https://doi.org/10.1016/j.drup.2004.01.004

Perillo, B., Di Donato, M., Pezone, A., Di Zazzo, E., Giovannelli, P., Galasso, G., Castoria, G., & Migliaccio, A. (2020, Feb). ROS in cancer therapy: the bright side of the moon. *Exp Mol Med, 52*(2), 192-203. https://doi.org/10.1038/s12276-020-0384-2

Perry, J. R., Laperriere, N., O'Callaghan, C. J., Brandes, A. A., Menten, J., Phillips, C., Fay, M., Nishikawa, R., Cairncross, J. G., Roa, W., Osoba, D., Rossiter, J. P., Sahgal, A., Hirte, H., Laigle-Donadey, F., Franceschi, E., Chinot, O., Golfinopoulos, V., Fariselli, L., Wick, A., Feuvret, L., Back, M., Tills, M., Winch, C., Baumert, B. G., Wick, W., Ding, K., & Mason, W. P. (2017, Mar 16). Short-Course Radiation plus Temozolomide in Elderly Patients with Glioblastoma. *N Engl J Med, 376*(11), 1027-1037. https://doi.org/10.1056/NEJMoa1611977

Rae, C., Tesson, M., Babich, J. W., Boyd, M., Sorensen, A., & Mairs, R. J. (2013, Jun). The role of copper in disulfiram-induced toxicity and radiosensitization of cancer cells. *J Nucl Med, 54*(6), 953-960. https://doi.org/10.2967/jnumed.112.113324

Rasper, M., Schäfer, A., Piontek, G., Teufel, J., Brockhoff, G., Ringel, F., Heindl, S., Zimmer, C., & Schlegel, J. (2010, Oct). Aldehyde dehydrogenase 1 positive glioblastoma cells show brain tumor stem cell capacity. *Neuro Oncol, 12*(10), 1024-1033. https://doi.org/10.1093/neuonc/noq070

Robert Koch-Institut, G. d. e. K. i. D. e. V. (2019, Version as of 17/08/2020). Krebs in Deutschland für 2015/2016. *Krebs in Deutschland 12*. https://doi.org/doi:10.25646/5977.3

Schäfer, A., Teufel, J., Ringel, F., Bettstetter, M., Hoepner, I., Rasper, M., Gempt, J., Koeritzer, J., Schmidt-Graf, F., Meyer, B., Beier, C. P., & Schlegel, J. (2012, Dec). Aldehyde dehydrogenase 1A1--a new mediator of resistance to temozolomide in glioblastoma. *Neuro Oncol, 14*(12), 1452-1464. https://doi.org/10.1093/neuonc/nos270

Schwartzbaum, J. A., Fisher, J. L., Aldape, K. D., & Wrensch, M. (2006, Sep). Epidemiology and molecular pathology of glioma. *Nat Clin Pract Neurol, 2*(9), 494-503; quiz 491 p following 516. https://doi.org/10.1038/ncpneuro0289

Sia, J., Szmyd, R., Hau, E., & Gee, H. E. (2020). Molecular Mechanisms of Radiation-Induced Cancer Cell Death: A Primer. *Front Cell Dev Biol, 8*, 41. https://doi.org/10.3389/fcell.2020.00041

Sies, H., & Cadenas, E. (1985, Dec 17). Oxidative stress: damage to intact cells and organs. *Philos Trans R Soc Lond B Biol Sci, 311*(1152), 617-631. https://doi.org/10.1098/rstb.1985.0168

Stummer, W., Pichlmeier, U., Meinel, T., Wiestler, O. D., Zanella, F., & Reulen, H. J. (2006, May). Fluorescence-guided surgery with 5-aminolevulinic acid for resection of malignant glioma: a randomised controlled multicentre phase III trial. *Lancet Oncol, 7*(5), 392-401. https://doi.org/10.1016/s1470-2045(06)70665-9

Stupp, R., Hegi, M. E., Mason, W. P., van den Bent, M. J., Taphoorn, M. J., Janzer, R. C., Ludwin, S. K., Allgeier, A., Fisher, B., Belanger, K., Hau, P., Brandes, A. A., Gijtenbeek, J., Marosi, C., Vecht, C. J., Mokhtari, K., Wesseling, P., Villa, S., Eisenhauer, E., Gorlia, T., Weller, M., Lacombe, D., Cairncross, J. G., & Mirimanoff, R. O. (2009, May). Effects of radiotherapy with concomitant and adjuvant temozolomide versus radiotherapy alone on survival in glioblastoma in a randomised phase III study: 5-year analysis of the EORTC-NCIC trial. *Lancet Oncol, 10*(5), 459-466. https://doi.org/10.1016/s1470-2045(09)70025-7

Stupp, R., Taillibert, S., Kanner, A., Read, W., Steinberg, D., Lhermitte, B., Toms, S., Idbaih, A., Ahluwalia, M. S., Fink, K., Di Meco, F., Lieberman, F., Zhu, J. J., Stragliotto, G., Tran, D., Brem, S., Hottinger, A., Kirson, E. D., Lavy-Shahaf, G., Weinberg, U., Kim, C. Y., Paek, S. H., Nicholas, G., Bruna, J., Hirte, H., Weller, M., Palti, Y., Hegi, M. E., & Ram, Z. (2017, Dec 19). Effect of Tumor-Treating Fields Plus Maintenance Temozolomide vs Maintenance Temozolomide Alone on Survival in Patients With Glioblastoma: A Randomized Clinical Trial. *Jama, 318*(23), 2306-2316. https://doi.org/10.1001/jama.2017.18718

Szatrowski, T. P., & Nathan, C. F. (1991, Feb 1). Production of large amounts of hydrogen peroxide by human tumor cells. *Cancer Res, 51*(3), 794-798.

Trachootham, D., Alexandre, J., & Huang, P. (2009, Jul). Targeting cancer cells by ROS-mediated mechanisms: a radical therapeutic approach? *Nat Rev Drug Discov, 8*(7), 579-591. https://doi.org/10.1038/nrd2803

Vasiliou, V., Bairoch, A., Tipton, K. F., & Nebert, D. W. (1999, Aug). Eukaryotic aldehyde dehydrogenase (ALDH) genes: human polymorphisms, and recommended nomenclature based on divergent evolution and chromosomal mapping. *Pharmacogenetics, 9*(4), 421-434.

Vasiliou, V., & Nebert, D. W. (2005, Jun). Analysis and update of the human aldehyde dehydrogenase (ALDH) gene family. *Hum Genomics, 2*(2), 138-143. https://doi.org/10.1186/1479-7364-2-2-138

Venkatesh, K. S., & Ramanujam, P. (2002, Apr). Endoscopic therapy for radiation proctitis-induced hemorrhage in patients with prostatic carcinoma using argon plasma coagulator application. *Surg Endosc, 16*(4), 707-710. https://doi.org/10.1007/s00464-001-8164-0

Volotskova, O., Hawley, T. S., Stepp, M. A., & Keidar, M. (2012). Targeting the cancer cell cycle by cold atmospheric plasma. *Sci Rep, 2*, 636. https://doi.org/10.1038/srep00636

Walk, R. M., Snyder, J. A., Srinivasan, P., Kirsch, J., Diaz, S. O., Blanco, F. C., Shashurin, A., Keidar, M., & Sandler, A. D. (2013, Jan). Cold atmospheric plasma for the ablative treatment of neuroblastoma. *J Pediatr Surg, 48*(1), 67-73. https://doi.org/10.1016/j.jpedsurg.2012.10.020

Wang, J., Yang, C. L., & Zou, L. L. (2017, Nov). Aldehyde dehydrogenase 1 expression has prognostic significance in patients with glioma. *Mol Clin Oncol, 7*(5), 885-890. https://doi.org/10.3892/mco.2017.1396

Wick, W., Bendszus, M., Goldbrunner, R., Grosu, A., Hattingen, E., Hau, P., Herrlinger, U., Kessler, T., Platten, M., Pukrop, T., Reifenberger, G., Sahm, F., Schaaf, S., Schlegel, U., Steinbach, J., Stockhammer, G., Stummer, W., Tabatabai, G., Tonn, J. C., & Weller, M. (2021). Gliome, S2k-Leitlinie. Retrieved 18/01/2022, from www.dgn.org/leitlinien

Wu, W., Wu, Y., Mayer, K., von Rosenstiel, C., Schecker, J., Baur, S., Würstle, S., Liesche-Starnecker, F., Gempt, J., & Schlegel, J. (2020, Mar). Lipid Peroxidation Plays an Important Role in Chemotherapeutic Effects of Temozolomide and the Development of Therapy Resistance in Human Glioblastoma. *Transl Oncol, 13*(3), 100748. https://doi.org/10.1016/j.tranon.2020.100748

Xu, X., Chai, S., Wang, P., Zhang, C., Yang, Y., Yang, Y., & Wang, K. (2015, Dec 1). Aldehyde dehydrogenases and cancer stem cells. *Cancer Lett, 369*(1), 50-57. https://doi.org/10.1016/j.canlet.2015.08.018

Yan, D., Sherman, J. H., & Keidar, M. (2017, Feb 28). Cold atmospheric plasma, a novel promising anti-cancer treatment modality. *Oncotarget, 8*(9), 15977-15995. https://doi.org/10.18632/oncotarget.13304

Yan, D., Talbot, A., Nourmohammadi, N., Sherman, J. H., Cheng, X., & Keidar, M. (2015, Dec 22). Toward understanding the selective anticancer capacity of cold atmospheric plasma--a model based on aquaporins (Review). *Biointerphases, 10*(4), 040801. https://doi.org/10.1116/1.4938020

Yan, X., Xiong, Z., Zou, F., Zhao, S., Lu, X., Yang, G., He, G., & Ostrikov, K. K. (2011). Plasma-Induced Death of HepG2 Cancer Cells: Intracellular Effects of Reactive Species. *Plasma Process Polym, 9*(1), 59-66. https://doi.org/10.1002/ppap.201100031

Yan, X., Zou, F., Zhao, S., Lu, X., He, G., Xiong, Z., Xiong, Q., Zhao, Q., Deng, P., Huang, J., & Yang, G. (2010). On the Mechanism of Plasma Inducing Cell Apoptosis. *IEEE Transactions On Plasma Science, 38*(9), 2451-2457. https://doi.org/10.1109/TPS.2010.2056393